# Transition Metal Hydrides

Biomimetic Studies and Catalytic Applications

**Jesper Ekström**


Stockholm University

ISBN 978-91-7155-539-7

Printed in Sweden by US-AB, Stockholm 2007
Distributor: Department of Organic Chemistry

‘*Var som en anka brukade min mamma alltid säga. Håll dig lugn på ytan, och paddla utav bara helvete därunder.*’

Michael Caine

# Abstract

In this thesis, studies of the nature of different transition metal-hydride complexes are described. The first part deals with the enantioswitchable behaviour of rhodium complexes derived from amino acids, applied in asymmetric transfer hydrogenation of ketones. We found that the use of amino acid thio amide ligands resulted in the formation of the *R*-configured product, whereas the use of the corresponding hydroxamic acid- or hydrazide ligands selectively gave the *S*-alcohol.
Structure/activity investigations revealed that the stereochemical outcome of the catalytic reaction depends on the ligand mode of coordination.

In the second part, an Fe hydrogenase active site model complex with a labile amine ligand has been synthesized and studied. The aim of this study was to find a complex that efficiently catalyzes the reduction of protons to molecular hydrogen under mild conditions. We found that the amine ligand functions as a mimic of the loosely bound ligand which is part of the active site in the hydrogenase.
Further, an Fe hydrogenase active site model complex has been coupled to a photosensitizer with the aim of achieving light induced hydrogen production. The redox properties of the produced complex are such that no electron transfer from the photosensitizer part to the Fe moiety occurs.

In the last part of this thesis, the development of a protocol for the transfer hydrogenation of ketones to secondary alcohols without the involvement of transition metal catalysts is described. A variety of ketones were efficiently reduced in 2-propanol using catalytic amounts of alkali alkoxide under microwave irradiation.

# List of Publications

This thesis is based on the following papers, which will be referred to by Roman numerals:

**I** **A Simple and Efficient Catalyst System for the Asymmetric Transfer Hydrogenation of Ketones**
Katrin Ahlford, Alexey B. Zaitsev, Jesper Ekström, Hans Adolfsson
*Synlett* **2007**, 2541-2544

**II** **Asymmetric Transfer Hydrogenation of Ketones Catalyzed by Amino Acid Derived Rhodium Complexes – On the Origin of Enantioselectivity and Enantioswitchability**
Jesper Ekström, Katrin Ahlford, Alexey B. Zaitsev, Hans Adolfsson
*Preliminary manuscript*

**III** **Dynamic Ligation at the First Amine-coordinated Iron Hydrogenase Active Site Mimic**
Lennart Schwartz, Jesper Ekström, Reiner Lomoth, Sascha Ott
*Chemical Communications* **2006**, 4206-4208

**IV** **Bio Inspired Side-on Attachment of a Ruthenium Photosensitizer to an Iron Hydrogenase Active Site Model**
Jesper Ekström, Maria Abrahamsson, Carol Olson, Jonas Bergquist, Feliz B. Kanyak, Lars Eriksson, Licheng Sun, Björn Åkermark, Hans-Christian Becker, Leif Hammarström, Sascha Ott
*Dalton Transactions* **2006**, 4599-4606

**V** **A Simple and Efficient Catalytic Method for the Reduction of Ketones**
Jesper Ekström, Jenny Wettergren, Hans Adolfsson
*Advanced Synthesis and Catalysis* **2007**, *349*, 1609-1613

# Contents

# Abbreviations

The abbreviations are used in agreement with the standards of the subject.[1] Only nonstandard and unconventional ones that appear in the thesis are listed here.

| | |
|---|---|
| adt | azadithiolate, $SCH_2NRCH_2S$ |
| ATH | asymmetric transfer hydrogenation |
| Cys | cysteine |
| DPEN | 1,2-diphenylethylenediamine |
| Fc | ferrocene |
| P | photosensitizer |
| pdt | 1,3-propanedithiolate |
| SCE | standard calomel electrode |
| TH | transfer hydrogenation |
| tpy | 2,2':6',2''-terpyridine |
| Δ | heating |

[1] *J. Org. Chem.* **2007**, *72*, 23A-24A

# 1 Introduction

One of the first discovered organometallic complexes was $K[PtCl_3(C_2H_4)]\cdot H_2O$, also known as the Zeise salt.[2] This complex, prepared from $PtCl_2$ and ethanol, contains an interesting ethylene ligand, which is coordinated to the platinum with the π-electrons. The structure of this complex was debated and the definitive answer did not arrive until methods such as X-ray crystallography were developed.[3]

Organometallic complexes have been widely studied since the discovery of Zeise's salt. In the transformation of organic compounds, numerous transition metals reagents have been successfully applied. These can often be used under catalytic conditions, keeping the amount of metal waste and costs down.

With partly filled d orbitals, the transition metals are in the twilight zone between organic and inorganic chemistry, and have properties that make them able to react in ways that are impossible for regular organic reagents. Organometallic reagents are often highly selective, and in principle it is possible to find a metal complex that can coordinate to any conceivable functional group. When coordinating, the metal can change the reactivity of the functional group. For instance they can make electrophilic groups nucleophilic or vice versa, stable groups reactive or stabilize reactive groups. In this way various reactions can be performed in the presence of otherwise reactive functional groups. With these abilities, the use of transition metal catalysis is a good complement to classical synthetic organic methods. A huge number of different reactions have been performed using different transition metal catalysts, and the 2005 year Nobel prize award to Grubbs, Schrock and Chauvin for the metathesis reaction proves that organometallic catalysis is a topic in focus.

## 1.1 Metal hydrides

The formal definition of a hydride is the negative ion of hydrogen, $H^-$. Hydrides themselves do only exist under extreme conditions, but the name is

[2] Zeise, W. C. *Annalen der Physik und Chemie* **1831**, *97*, 497-541

[3] a) Wunderlich, J. A.; Mellor, D. P. *Acta Cryst.* **1955**, *8*, 57.; b) Black, M.; Mais, R. H. B.; Owston, P. G. *Acta Cryst.* **1969**, *B25*, 1753-1759

often used when referring to compounds with a hydrogen bound to an atom with lower electronegativity than hydrogen. Depending on the nature of the bonding atom, the hydrides are sorted into different classes. Transition metal hydrides are key intermediates in reactions such as homogeneous hydrogenation, hydroformylation, hydrometallation and transfer hydrogenation.

The reactivity of the transition metal hydrides depends on the properties of the metal and the auxiliary ligands. The lower the electronegativity and the electron density at the metal, the more polar and ionic will the bond to the hydride be. With an ionic bond between the metal and the hydride, it will have the properties of a classical hydride. The properties of the transition metal hydride can vary all the way from that of a hydride donor to that of a protic acid. Thus a wide span of hydrides with different reactivity can be generated.

The main focus in this thesis will be on transition metal hydrides; in the second chapter the application of rhodium hydrides in asymmetric transfer hydrogenation will be discussed. In the subsequent chapters, active site mimics of the Fe hydrogenase, which is an enzyme capable of generating iron-hydrides are presented. In the last chapter, direct hydride transfer reactions from hydrocarbons, without any transition metal intermediates will be discussed.

## 1.2 Transfer hydrogenation

The reduction of ketones to secondary alcohols is usually performed with the use of stoichiometric amounts of a hydride reagent such as $LiAlH_4$ or $NaBH_4$ or by the use of molecular hydrogen in combination with a transition metal catalyst. A disadvantage of these methods is the reactivity of the reagents which makes them problematic to store and handle. A method where this problem is avoided was discovered in the 1920's by Meerwein[4] and Verley.[5] They found that ketones could be reduced by aluminium ethoxide and ethanol. Ponndorf further refined the procedure and developed an effective method by using aluminium *iso*-propoxide and 2-propanol.[6] The reduction proceeds via a six-membered cyclic transition state, Scheme 1, which involves the ketone and the aluminium bound alkoxide.

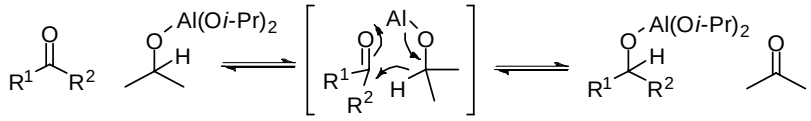


**Scheme 1.** The MVPO-reaction.

[4] Meerwein, H.; Schmidt, R. *Justus Liebigs Ann. Chem.* **1925**, *444*, 221-238
[5] Verley, M. *Bull. Soc. Chim. Fr.* **1925**, *37*, 871-874
[6] Ponndorf, W. *Angew. Chem.* **1926**, *39*,138-143

As illustrated in Scheme 1, a hydrogen transfer from a donor molecule, in this case the alkoxide, to the target ketone occurs. This type of reaction is hence called transfer hydrogenation.

In 1937, Oppenauer reported the oxidation of secondary alcohols in steroids using aluminium *tert*-butoxide.[7] This shows that when varying the reaction conditions, the reaction can be caused to proceed in either of the two directions and thus the equilibrium reaction is called the Meerwein-Verley-Ponndorf-Oppenauer (MVPO) reaction. A nice feature with the oxidation step is that overoxidation to the carboxylic acid is not possible due to the nature of the reaction.

In the 1960's transfer hydrogenation using transition metals was reported,[8] and in 1971 it was discovered that $RuCl_2(PPh_3)_3$ has catalytic activity in this process. This catalyst is slow though, and high temperature is needed to perform the reduction.[9] A major breakthrough was achieved when Chowdhury and Bäckvall found that the addition of base to the reaction mixture dramatically increased the catalytic activity of this complex.[10] The role of the base is to deprotonate the hydrogen donor alcohol to the alkoxide, which is necessary in order to activate the hydride shift from the donor to the metal.

2-Propanol and an azeotrope of formic acid and triethylamine (TEAF), 5:2, are the most frequently used hydrogen donors. When 2-propanol is used as hydrogen donor, acetone is formed as by-product. A drawback when running the reaction in 2-propanol is that there will be an equilibrium with the accumulated acetone. The reduction can be further pushed to the product side by removal of the formed acetone. This problem is completely avoided when TEAF is used as hydrogen donor. In this catalytic system, the formed byproduct, $CO_2$, leaves as a gas and thereby the reversible reaction is prohibited. Recently, the use of primary alcohols as hydrogen donor under non-reversible conditions were reported.[11]

## 1.3 Mechanistic pathways of the transfer hydrogenation

The transfer hydrogenation can proceed via various mechanisms. The mechanism proposed for the MVPO reaction (Scheme 1), involves a direct hydride transfer from the hydride donor to the acceptor, without any metal-hydride intermediate. This is the common mechanism for non-transition

[7] Oppenauer, R. V. *Recl. Trav. Chim. Pays-Bas.* **1937**, *56*, 137-144
[8] a) Bailar, J. C.; Itatani, H. *J. Am. Chem. Soc.* **1967**, *89*, 1592-1599; b) Trocha-Grimshaw, J.; Henbest, H. B. *Chem. Commun.* **1967**, 544
[9] Sasson, Y.; Blum, J. *Tetrahedron. Lett.* **1971**, 2167-2170
[10] Chowdhury, R. L.; Bäckvall, J. -E. *J. Chem. Soc., Chem. Commun.* **1991**, 1063-1064
[11] Maytum, H. C.; Tavassoli, B.; Williams, J. M. J. *Org. Lett.* **2007**, *9*, 21, 4387-4389

metals. For transition metals, the reduction usually proceeds via a metal hydride intermediate. Either a mono-hydride or a di-hydride route is possible. Complexes **1** and **2** represent two different types of ruthenium complexes that can be used as catalysts in transfer hydrogenation reactions. In complex **2** an aromatic ligand is coordinated to the metal. The complex is catalytically active in combination with different bidentate ligands.

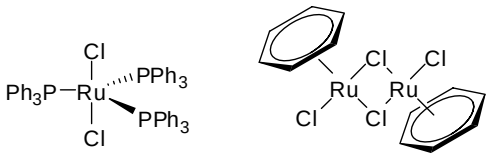


**1** **2**

**Figure 1.** Two types of ruthenium complexes used in transfer hydrogenation.

For ruthenium complexes, the mono-hydride route is commonly occurring for cyclopentadienyls and arene half-sandwich complexes.[12] Simpler complexes usually react via the di-hydride route (Scheme 2, I). The generation of the metal di-hydride takes place in two steps.[13] First, the alkoxide displaces a ligand at the metal, and then the first hydride is formed through β-hydride elimination. The same procedure is repeated to form the reactive di-hydride complex. There are two different types of mono-hydride reaction mechanisms. The reaction either proceeds via a metal alkoxide intermediate, where the hydride is transferred after coordination with the metal (this path is called inner-sphere, Scheme 2, II) or it can take place without coordination of the donor and substrate to the metal (called outer-sphere, Scheme 2, III)

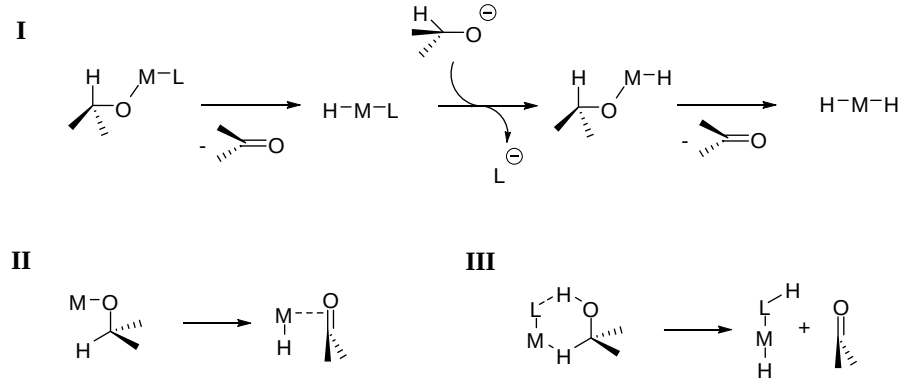


**Scheme 2.** The di-hydridic (I), the mono-hydridic inner-sphere (II) and the mono-hydridic outer-sphere (III) mechanisms.

[12] a) Pàmies, O.; Bäckvall, J. -E. *Chem. Eur. J.* **2001**, *7*, 5052-5058; b) Samec, J. S. M.; Bäckvall, J. -E.; Andersson, P. G.; Brandt, P. *Chem. Soc. Rev.* **2006**, *35*, 237-248

[13] Laxmi, Y. R. S.; Bäckvall, J. -E. *Chem. Commun.* **2000**, 611-612

## 1.4 Asymmetric transfer hydrogenation

We all live in a chiral environment. Chirality spans from the cars we drive and the clothes we wear to the molecules that we are made of. Enantiomers are two mirror images of the same molecule that are not superimposable. In an achiral environment, they have the same physical properties, except that they rotate plane polarized light in opposite directions. However, in a chiral environment, like in our bodies, enantiomers will interact differently. Where one enantiomer interacts in one way, the other can be unreactive or may interact in a different way. In order to avoid undesired side-reactions, it is therefore often necessary to have enantiomerically pure substances.

There are several different strategies available for the synthesis of enantiomerically pure compounds. Material can be isolated from natural sources, also called the chiral pool. Such compounds can be used directly, or be used as starting material for further synthesis. Enantiomerically pure material can also be made through resolution of a racemate or it can be made through asymmetric synthesis. Several approaches are available for asymmetric synthesis; the asymmetry can be induced by a stereocenter in the substrate or by an auxiliary. Another approach is to use chiral reagents, or the enantiomerically enriched compounds can be obtained through asymmetric catalysis.

The first part of this thesis concentrates on an asymmetric catalytic reaction; the asymmetric transfer hydrogenation of prochiral ketones. Early examples of asymmetric transfer hydrogenation involved aluminium alkoxides in combination with chiral donors in classic MVPO reactions.[14] However, the results obtained with these protocols were poor. A more successful strategy has been the use of chiral catalysts for hydrogen transfer. Some of the first reported systems involved Ru, Rh and Ir in combination with chiral phosphine ligands.[15,16,17] The equilibrium beween the product alcohol and acetone formed from 2-propanol caused racemization, so the conversions and enantioselectivities for these systems were still generally low.

Significantly better results were obtained after Bäckvall discovered the improved reactivity upon addition of base, and an *ee* of 93% was reported for the reduction of acetophenone in 2-PrOH using a ruthenium complex of ligand **3**. Running the reaction with various α-amino alcohols like ephedrine **4** and 2-amino-1,2-diphenylethanols with ruthenium arenes gave good enantioselectivity and high conversion with short reaction times.[18] Half-sandwich complexes, such as Ru-arenes and Rh or Ir-cyclopentadienyl complexes are

---

[14] Doering, W. E.; Young, R. W. *J. Am. Chem. Soc.* **1950**, *72*, 631
[15] Bianchi, M.; Matteoli, U.; Menchi, G.; Frediani, P.; Pratesi, S.; Pianceti, F.; Botteghi, C. *J. Organomet. Chem.* **1980**, *198*, 73-80
[16] Spogliarichi, R.; Kaspar, J.; Graziani, M.; Morandini, F. *J. Organomet. Chem.* **1986**, *306*, 407-412
[17] Krause, H. W.; Bhatnagar, A. K. *J. Organomet. Chem.* **1986**, *302*, 265-267
[18] Takehara, J.; Hashiguchi, S.; Fujii, A.; Inoue, S.; Ikariya, T.; Noyori, R. *Chem. Commun.* **1996**, 233-234

the transition metal fragment that has been most successfully used in combination with amino alcohols and diamines. The arene or cyclopentadienyl occupies three coordination sites at the metal, leaving three unoccupied and also forcing a bidentate ligand to coordinate in a *fac* manner. When a chiral ligand is coordinated to a transition metal arene or cyclopentadienyl complex, the metal can become a stereocenter.

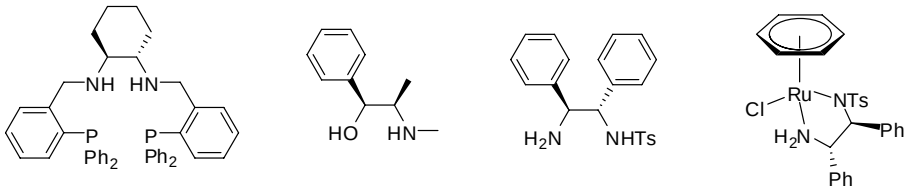


**3** **4** **5** **6**

**Figure 2.**

The most successful ligand used so far for the asymmetric transfer hydrogenation is Noyori's mono-tosylated diamine (TsDPEN) ligand **5**.[19] In combination with ruthenium arenes this ligand forms a stable complex, **6**, which catalyzes the reduction of ketones and imines to alcohols and amines with excellent conversion and *ee*. The TsDPEN-Ru complex is bifunctional; it contains one Lewis acidic and one Lewis basic site. The basic site (the amine) deprotonates the hydrogen donor which simultaneously transfers a hydride to the Lewis acidic Ru (mechanism type III, Scheme 2). In 2-PrOH, this catalyst performs at the same level as the α-amino alcohols, but in TEAF, full conversion and higher *ee*'s are obtained.[20] A drawback is that the latter catalytic system is rather slow and longer reaction times are needed.

## 1.5 Metalloenzymes

Over billions of years, nature has developed efficient and selective catalysts that are active under mild conditions. Of the known proteins, about 40% contain metal ions.[21] The metal can be a co-factor or incorporated in the protein structure. The most commonly occurring metals in the active sites are Mn, Fe, Cu and Zn. In the same way as in synthetic organic chemistry, enzymes use transition metals to perform difficult reactions. For example,

[19] Noyori, R.; Hashiguchi, S. *Acc. Chem. Res.* **1997**, *30*, 97-102
[20] Fujii, A.; Hashiguchi, S.; Uematsu, N.; Ikariya, T.; Noyori, R. *J. Am. Chem. Soc.* **1996**, *118*, 2521-2522
[21] a) Noodleman, L.; Lovell, T.; Han, W. -G.; Li, J.; Himo, F. *Chem. Rev.* **2004**, *104*, 459-508; b) Castagnetto, J. M.; Hennessy, S. W.; Roberts, V. A.; Getzoff, E. D.; Tainer, J. A.; Pique, M. E. *Nucleic Acids Res.* **2002**, *30*, 379-382

manganese participates in the water oxidation in photosystem II,[22] iron is part of the active site in the nitrogenases, which catalyze the fixation of $N_2$,[23] and the hydrogenases which consume or produce $H_2$.[24] In the enzyme superoxide dismutase, an oxygen radical is turned into oxygen and hydrogen peroxide using copper,[25] and zinc is found in the active site of alcohol dehydrogenase, which oxidizes ethanol to acetaldehyde.[26]

When developing new catalysts, inspiration and knowledge can be gained through studies of nature's catalytic systems. Due to our interest in reduction chemistry, we were intrigued by the remarkable properties of the hydrogenases.

## 1.6 Hydrogenases

Microorganisms have developed effective ways of using hydrogen as an electron source. The oxidation of hydrogen to protons and reduction of protons to hydrogen is catalyzed by a family of enzymes called the hydrogenases.[27] The hydrogenases are divided into subclasses depending on the metal cations in their active site; NiFe, Fe and a class of hydrogenases previously believed to be without metals in the active site.[28]

The Fe hydrogenases mainly catalyze the reduction of protons to molecular hydrogen whereas the NiFe hydrogenases are more efficient in oxidation of hydrogen.

In the late nineties, Peters et. al and Nicolet et. al reported the crystal structures of the Fe hydrogenases from *Clostridium pasteurianum*[29] and *Desulfovibrio desulfuricans*.[30]

The active site, called the H-cluster, is buried deeply within the enzyme. A pathway of amino acid sidechains capable of proton exchange makes proton transfer to the active site possible and channels for $H_2$ transfer have also been found.

---

[22] a) Ferreira K. N.; Iverson T. M.; Maghlaoui K.; Barber J.; Iwata, S. *Science* **2004**, *303*, 1831-4026; b) Barber, J. *Biochem. Soc. Trans.* **2006**, *34*, 619–631

[23] Sellman, D.; Utz, J; Heinemann, F. W. *Coord. Chem. Rev.* **1999**, *190-192*, 607-627

[24] Adams, M. W. W. *Biochim. Biophys. Acta.* **1990**, *1020*, 115-145

[25] Bertini, I.; Felli, I. C.; Luchinat, C.; Parigi, G.; Pierattelli, R. *ChemBioChem* **2007**, *8*, 1422-1429

[26] a) Kleifeld, O.; Frenkel, A.; Martin, J. M. L.; Sagi, I. *Nature Structural Biology* **2003**, *10*, 98-103; b) Esposito, L.; Sica, F.; Raia, C. A.; Giordano, A.; Rossi, M.; Mazzarella, L.; Zagari, A. *J. Mol. Biol.* **2002**, *318*, 463-477

[27] Frey, M. *ChemBioChem* **2002**, *3*, 153-160

[28] a) Darensbourg, M. Y.; Lyon, E. J.; Smee, J. J. *Coord. Chem. Rev.* **2000**, 206-207, 533-561; b) Shima, S.; Lyon, E. J.; Thauer, R. K.; Mienert, B.; Bill, E. *J. Am. Chem. Soc.* **2005**, *127*, 10430-10435

[29] Peters, J. W.; Lanzilotta, W. N.; Lemon B. J.; Seefeldt, L. C. *Science* **1998**, *282*, 1853-1858

[30] Nicolet, Y.; Piras, C.; Legrand, P.; Hatchikian, E. C.; Fontecilla-Camps, J. C. *Structure* **1999**, *7*, 13-23

The H-cluster, Figure 3a, contains six Fe atoms. A cubic $[Fe_4S_4]$ cluster is linked through a cysteinyl sulfur to a dinuclear Fe complex, which is believed to be the catalytic center where the reduction takes place. The two Fe atoms (referred to as proximal, $Fe_p$ and distal, $Fe_d$ with respect to the cysteine) have a Fe-Fe bond distance of 2.62 Å and are linked by a dithiolate ligand, first identified as propanedithiolate, pdt, but later believed to be an azadithiolate, adt.[31] The Fe nuclei are coordinated by biologically very unusual CO and CN ligands, normally associated with inhibition and poisoning. At the distal iron, another ligand, believed to be $H_2O$ or $^-OH$ is found. The H-cluster is further anchored to the protein scaffold through hydrogen bonding interactions between the CNs and the polypeptide.

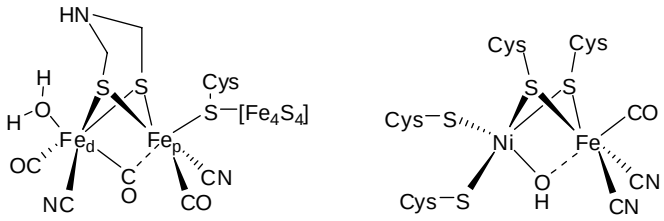


a) b)

**Figure 3.** a) The H-cluster b) The active site of the NiFe hydrogenase.[32]

Although the enzymes are biologically nonrelated, the H-cluster and the active site of the NiFe hydrogenase, Figure 3b, have many common features. Different ways of superimposing the two active sites show that the distal iron in the H-cluster and the iron in the NiFe have almost the same coordination spheres.[31,33] Both these complexes contain a labile ligand which enables the coordination of substrate molecules to the metals. The CO and CN ligands stabilize metals in low oxidation states. The electron rich iron is capable of doing an oxidative addition of a proton, resulting in the formal oxidation of the metal and the formation of an iron-hydride. These properties make these two active sites suitable environments for proton reduction.

[31] Nicolet, Y.; de Lacey, A. L.; Vernède, X.; Fernandez, E. C.; Hatchikian, E. C.; Fontecilla-Camps, J. C. *J. Am. Chem. Soc.* **2001**, *123*, 1596-1601
[32] Volbeda, A.; Charon, M. -H.; Piras, C.; Hatchikian, E. C.; Frey, M.; Fontecilla-Camps, J. C. *Nature* **1995**, *373*, 580-587
[33] Brusci, M.; Zampella, G; Fantucci, P.; De Gioia, L. *Coord. Chem. Rev.* **2005**, *249*, 1620-1640

## 1.7 The aim of this thesis

The aim of this work was to develop new asymmetric transfer hydrogenation protocols using rhodium cyclopentadienyls and chiral ligands derived from amino acids as catalysts, and to study the properties of these complexes.

A further aim was to study the properties and reactivity of di-iron carbonyl complexes, which share features with the active site of the Fe-hydrogenase, an enzyme which catalyzes proton reduction. Further, the possibility to achieve light-induced proton reduction by coupling a hydrogenase model complex to a photosensitizer was investigated.

Finally, inspired by the reducing abilities of the hydrogenases, the goal was to develop a catalyst for ATH based on cheaper and more environmental benign metals.

# 2 Development of novel catalysts (Papers I & II)

Previously, the Adolfsson research group has developed catalysts for the asymmetric transfer hydrogenation of prochiral ketones using *in situ* formed Ru-half sandwich catalysts based on *pseudo*-dipeptide ligands derived from naturally available amino acids and amino alcohols (Scheme 3).[34] With these catalysts, aryl alkyl ketones are efficiently reduced with high stereocontrol.

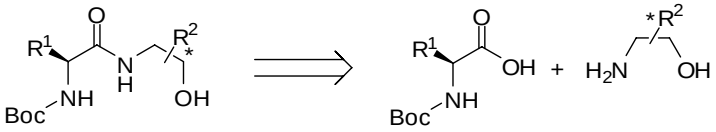


**Scheme 3.** The *pseudo*-dipeptide ligand, derived from an amino acid and an amino alcohol.

No ruthenium-*pseudo*-dipeptide complex has been isolated so far, thus the structure of the active catalyst is not known. However, a tridentate coordination between the *pseudo*-dipeptide ligand and the ruthenium has been suggested (Figure 4). The coordination is proposed to involve the nitrogen in the Boc-carbamate, the central amide and the alcohol. The amide and the alcohol are depicted as deprotonated and the Boc-carbamate is proposed to coordinate the metal as a neutral ligand. These three functional groups are important, and when removed or modified, the catalytic activity is lost.

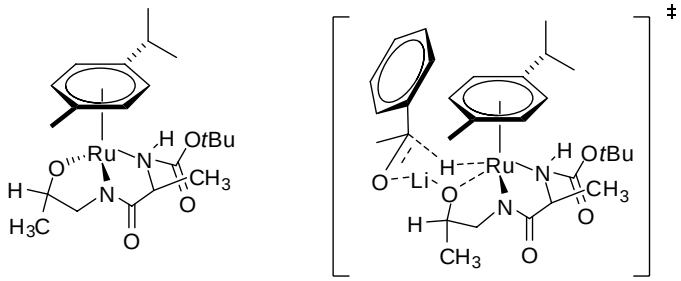


**Figure 4.** Proposed structure and transition state for the *pseudo*-dipeptide ruthenium catalyst.

[34] a) Pastor, I. M.; Västilä, P.; Adolfsson, H. *Chem. Commun.* **2002** 2046-2047; b) Pastor, I. M.; Västilä, P.; Adolfsson, H. *Chem. Eur. J.* **2003**, *9*, 4031-4045

In contrast to other ligands, the *pseudo*-dipeptides do not contain a basic nitrogen site. Instead, the alcohol functionality plays a crucial role during the catalytic cycle. The corresponding alkoxide functions as a basic site, and captures and delivers a proton during the hydrogen transfer. A positive effect on the activity and selectivity of the ruthenium-*pseudo*-dipeptide catalyst is noticed upon addition of $Li^+$ additives to the reaction mixture. The effect was the same when *i*-PrOLi was used as base. This effect is proposed to be a result of the tight six-membered ring transition state formed with the lithium cation (Figure 4).

The *pseudo*-dipeptide ligands contain two chiral centers, one on the amino acid part and one on the amino alcohol part. The product configuration is strongly correlated to the chiral center at the amino acid portion. When using a ligand derived from the *S*-amino acid, the *S*-enantiomer of the alcohol is obtained. The stereocenter at the amino alcohol portion has a less pronounced role, but it amplifies the enantioselectivity. In the initial study, primary amino alcohols were used, but better results were later reported with secondary amino alcohols.[35]

A problem with these complexes is the instability. The lifetime of the catalyst based on the *pseudo*-dipeptides is much shorter than that of Noyori´s TsDPEN-ruthenium catalyst. This could be due to several reasons, however the fact that no complex can be isolated indicates that the ligands coordinate poorly to the metal precursor. Furthermore, examination of the reaction mixture has shown that the amide bond is sensitive to cleavage. In an attempt to increase the stability of the complex, the amido functionality of the ligand was exchanged with a more acidic thio amide.[36] The switch did not result in any significant change in stability, but an interesting change in enantioselectivity occurred. Instead of the expected *S*-alcohol, the ruthenium catalyzed asymmetric transfer hydrogenation employing this ligand, resulted in the formation of the *R*-alcohol, Scheme 4.

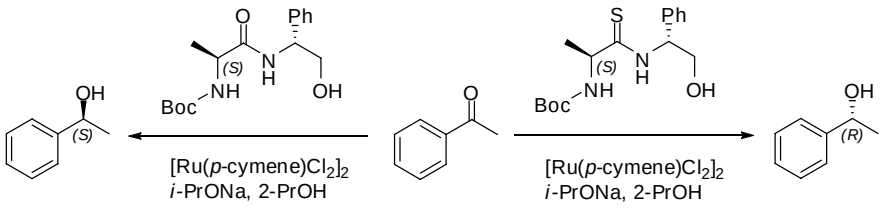


**Scheme 4.** The switch in enantioselectivity in the reduction of acetophenone.

It was later found that higher conversions and enantioselectivities were obtained when the alcohol functionality was omitted from the ligand structure and ruthenium was substituted with rhodium.

---

[35] Bøgevig, A.; Pastor, I. M.; Adolfsson, H. *Chem. Eur. J.* **2004**, *10*, 294-302
[36] Zaitsev, A. B.; Adolfsson, H. *Org. Lett.* **2006**, *8*, 5129-5132

## 2.1 Hydroxamic acid- and hydrazide ligands derived from amino-acids

The *pseudo*-dipeptide and thio amide ligands share many structural features, but there are some differences. While the *pseudo*-dipeptides are capable of coordinating in a tridentate fashion, the thio amides can only act as bidentate ligands. Another difference is, of course, the presence of the thio amide instead of the amide functionality in the thio amide ligand. The effect when going from an amide to a thio amide is that the acidity of the amide proton is increased (Figure 5).

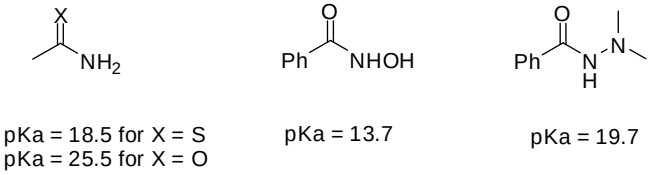


**Figure 5.** Representative pKa values of amides, thio amides, hydroxamic acids and hydrazides (DMSO).[37]

To investigate whether the enantioswitchable behaviour is a consequence of the ligand acidity, we decided to affect the acidity of the amide NH bond without replacing the carbonyl oxygen with sulfur. This can be accomplished by the introduction of an electron-withdrawing group on the amide. Starting from the *N*-Boc protected amino acid, there are a few ways to perform this structural change. For instance, the carboxylic acid can be converted to a hydroxamic acid or a hydrazide.

*N*-Boc protected amino acids were converted to hydroxamic acids following a procedure developed by Giacomelli et. al (Scheme 5).[38]

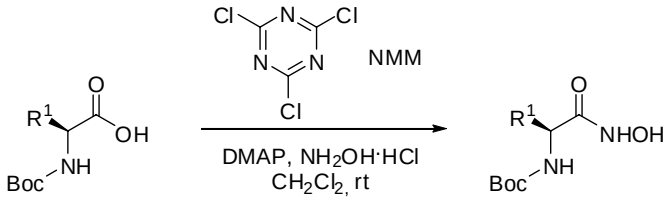


**Scheme 5.** One-pot procedure for the formation of the hydroxamic acid ligands.

Using this procedure, we prepared the ligands **7a**-**e**. We were, however, not able to reproduce the reported yields obtained by Giacomelli.

[37] These data were extracted from the table at http://www.chem.wisc.edu/areas/reich/pkatable/
[38] Giacomelli, G.; Porcheddu, A.; Salaris, M. *Org. Lett.* **2003**, *5*, 2715-2717

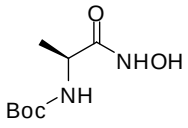

**7a**

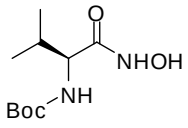

**7b**

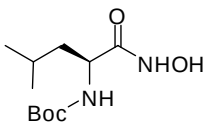

**7c**

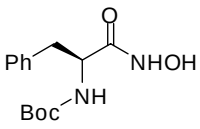

**7d**

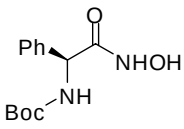

**7e**

The hydrazides **8a-d** were prepared using NMM and *iso*-butyl chloroformate according to the procedure presented in Scheme 6.

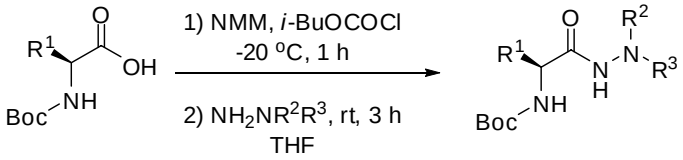


**Scheme 6.** One-pot procedure for the formation of the hydrazide ligands.

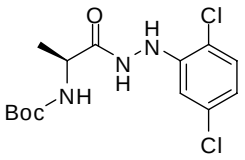

**8a**

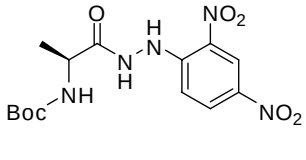

**8b**

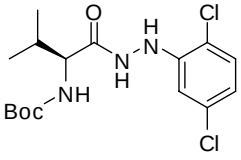

**8c**

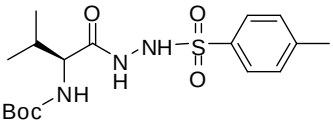

**8d**

## 2.2 Ligand screening

When employing the alanine derived hydroxamic acid **7a** in the rhodium catalyzed transfer hydrogenation of acetophenone using conditions as described in Scheme 7, a conversion of 66% and an *ee* of 82% (*S*) was obtained after 30 minutes (see Table 1). Prolonged reaction time leads to higher conversion but lower *ee*. For the catalytic system based on the *pseudo*-dipeptides, a positive effect was noticed when LiCl was added. In agreement with these previous observations on the *pseudo*-dipeptide system, addition of LiCl (5 mol%) to the hydroxamic acid catalytic system, results in higher *ee* (88%). When using the valine derived ligand **7b**, an even higher *ee* (97%) was obtained. For the leucine ligand **7c**, lower conversion (53%) and *ee* (77%) was noticed, whereas it was only slightly lower, (63% yield, 92% *ee*) for the phenylalanine ligand **7d**. High conversion, but poor enantioselectivity was obtained using the phenylglycine ligand **7e**. From these results it can be concluded that the valine based ligand **7b** shows the most promising results and that in contrast to the thio amide ligands, the (*S*)-enantiomer of the phenylethanol is formed in excess.

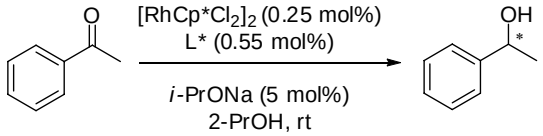


**Scheme 7.** Reaction conditions for the ruthenium catalyzed asymmetric reduction of acetophenone.

**Table 1:** Catalytic results employing the hydroxamic acid ligands **7a-e**.[a]

| Entry | Ligand | LiCl (5 mol%) | Time [h] | Conversion [%] | *ee* [%] |
|---|---|---|---|---|---|
| **1** | **7a** | - | 0.5 | 66 | 82 |
| **2** | **7a** | + | 0.5 | 56 | 88 |
| **3** | **7b** | - | 2 | 89 | 87 |
| **4** | **7b** | + | 2 | 82 | 97 |
| **5** | **7c** | - | 2 | 44 | 77 |
| **6** | **7c** | + | 2 | 53 | 77 |
| **7** | **7d** | - | 2 | 45 | 86 |
| **8** | **7d** | + | 2 | 63 | 92 |
| **9** | **7e** | - | 2 | 95 | 12 |

a) For reaction conditions, see Scheme 7 and Paper I.

The catalyst formed when using the hydrazide ligands together with rhodium is slightly less reactive than the hydroxamic acid catalyst, and the conversions are generally lower than those obtained with the hydroxamic acid ligands. A conversion of 43% and an *ee* of 80% (*S*) were obtained using **8a**. When the valine derived ligand **8c**, which is bulkier, was employed, lower activity (20%), but slightly higher enantioselectivity (84%) was obeserved. Adding LiCl (5 mol%) to these catalytic systems, in contrast to the hyroxamic acid case, results in a drop in both conversion and enantioselectivity.

Having a more electron-withdrawing substituent on the amide as in the alanine derived ligand **8b**, results in lower conversion (30%), but similar *ee* (81%) as with **8a**. When a more electron-withdrawing substituent is placed on the amide in the valine derived ligand **8d**, both activity (9%) and selectivity (28%) is poor.

Both when using the hydroxamic acids and the hydrazides as ligands, the (*S*)-enantiomer of the phenylethanol is formed in excess. Thus it seems as if it is the presence of the thio amide rather than the increased acidity of the amide proton that is the reason behind the observed enantio-switch.

**Table 2.** Catalytic results employing the hydroxamic acid ligands **8a-d**.[a]

| Entry | Ligand | LiCl (5 mol%) | Time [h] | Conversion [%] | *ee* [%] |
|---|---|---|---|---|---|
| **1** | **8a** | - | 2 | 43 | 80 |
| **2** | **8a** | + | 2 | 9 | 49 |
| **3** | **8b** | - | 2 | 30 | 81 |
| **4** | **8b** | + | 2 | 56 | 91 |
| **5** | **8c** | - | 2 | 20 | 84 |
| **6** | **8c** | + | 2 | 7 | 50 |
| **7** | **8d** | - | 2 | 9 | 28 |
| **8** | **8d** | + | 2 | 5 | 11 |

a) For reaction conditions, see Scheme 7 and Paper II.

## 2.3 Ligand coordination in the active catalyst

The hydroxamic acid and thio amide ligands share the amino acid core and the carbamate protecting group. The difference between these two types of ligands is the functional group at the *C*-terminal. A closer look on the coordinating abilities of the hydroxamic acid and thio amide ligands might reveal the reason behind the enantioswitch. There are several possibilities in which the hydroxamic acid and thio amide ligand can bind to the metal (Figure 6).

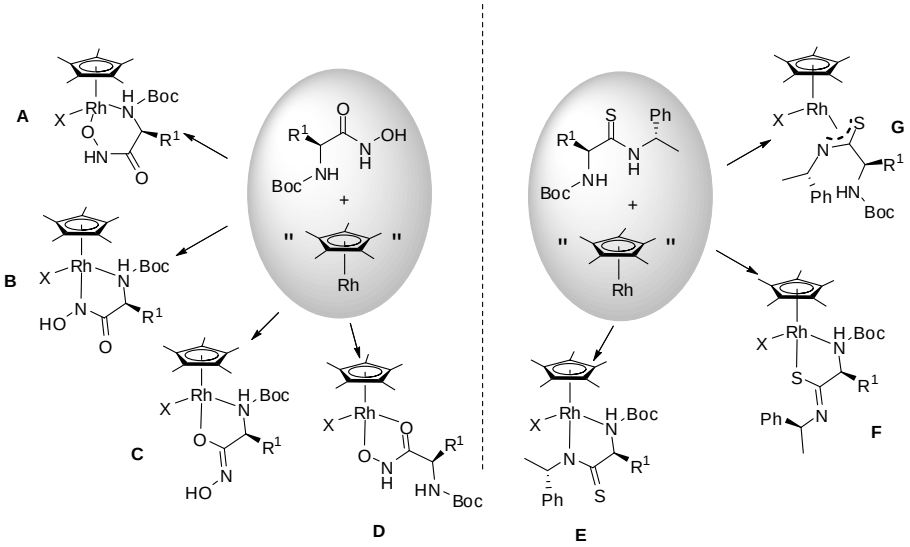


**Figure 6.** Possible coordination modes for *N*-Boc protected amino acid derived hydroxamic acid and thio amide ligands in combination with Rh-cyclopentadienyl.

Simple hydroxamic acid ligands coordinate transition metals in a chelating manner (Figure 6, **D**).[39] In an amino acid derived hydroxamic acid ligand, it is also possible for the Boc carbamate nitrogen to coordinate together with the hydroxamide acid part (Figure 6, **A**, **B** or **C**). Another possibility is for the Boc-carbamate to coordinate with the carbonyl oxygen. This is less likely however, since the chelate ring created would be large and energetically unfavored.

In the case of the thio amide ligands, there are three hetero atoms that may coordinate to the metal, the nitrogen in the Boc carbamate, the nitrogen in the thio amide and the sulfur in the thio amide function. The coordination is most likely a chelation between the Boc-carbamate nitrogen and either the nitrogen (Figure 6, **E**) or the sulfur (Figure 6, **F**) in the thio amide. It is also

[39] a) Farkas, E.; Enyedy, É. A.; Micera, G.; Garribba, E. *Polyhedron* **2000**, *19*, 1726-1736;b) Milios, C. J.; Manessi-Zoupa, E.; Perlepes, S. P. *Trans. Met. Chem.* **2002**, *27*, 864-873 c) Hintermaier, F.; Helding, S.; Volodarsky, L. B.; Sünkel, K.; Polborn, K.; Beck, W. *Z. Naturforsch.* **1998**, *53 b*, 101-109; d) Farkas, E.; Csóka, H. *J. Inorg. Biochem.* **2002**, *89*, 219-226

possible for the thio amide function to coordinate the rhodium in a $\eta^3$-manner (Figure 6, **G**).

In order to get information about the structure of the hydroxamic acid-rhodium complex, it was studied by NMR spectroscopy. Due to the instability of the complex, no conclusion can be drawn from these experiments. Attempts to obtain crystallinic material suitable for X-ray analysis of the rhodium complexes with the hydroxamic acids and thio amides have also failed.

Another way of gaining knowledge of the ligand sphere around the active catalyst is by slightly modifying the ligand structure. From the impact of the modification on the activity and selectivity in the catalytic experiments, conclusions on the importance of the ligand structure can be drawn.

### 2.3.1 Coordination of the hydroxamic acid ligand

By employing ligand **9**, synthesized from *S*-(+)-phenyl butyric acid, under the standard reaction conditions (Scheme 7) a conversion of 4% was obtained (Table 3). This poor result indicates that coordination with the Boc carbamate is necessary. By replacing the Boc-group at the nitrogen with a tosyl group as in **10**, the acidity of this site is significantly increased. This ligand does not show catalytic activity with the conditions presented in Scheme 7. However, upon addition of LiCl (5 mol%) to the reaction mixture, an interesting result is obtained. Now a conversion of 8% and an enantioselectivity of 53%, but this time of the (*R*)-product, were observed. In contrast to the *N*-Boc protected hydroxamic acid-catalysts, the most basic site in this complex, being protonated/deprotonated during the catalytic reaction, is presumably the hydroxamic acid function.

The activity is more or less lost when the carbamate group is removed (**12**). From these results it is clear that the activity of the complex is dependent on the properties of the proton at this position. In order to maintain high activity, it cannot be too acidic or basic. More puzzling is that the acetylated ligand **11**, does not show any activity. The changes when going from the Boc-carbamate to the acetylated ligand are small. The acidity of the proton is similar, and the structure is more or less the same. A reason behind this result might be that the nitrogen in the carbamate is a better donor molecule as compared to the nitrogen in the amide, because of the higher delocalization of the amide nitrogen lone-pair.[40]

[40] Basso, E. A.; Oliveira, P. R.; Wiectzycoski, F.; Pontes, R. M.; Fiorin, B. C. *J. Mol. Struct.* **2005**, *753*, 139-146

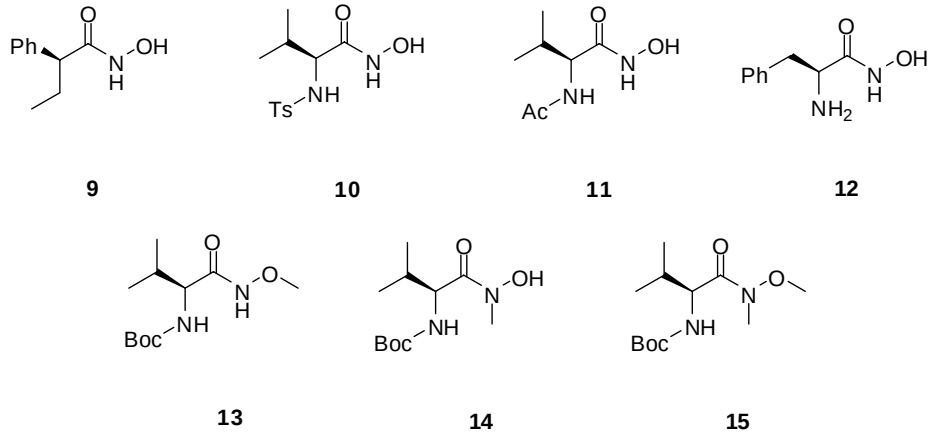


**Figure 7.**

**Table 3.** Catalytic results employing ligands **9**-**15**.[a]

| Entry | Ligand | LiCl (5 mol%) | Conversion [%] | *ee* [%] |
|---|---|---|---|---|
| **1** | **9** | - | 4 | - |
| **2** | **10** | - | 2 | - |
| **3** | **10** | + | 8 | 53(*R*) |
| **4** | **11** | - | 1 | - |
| **5** | **11** | + | 2 | 20(*S*) |
| **6** | **12** | - | 3 | - |
| **7** | **12** | + | 2 | - |
| **8** | **13** | - | 16 | 70(*S*) |
| **9** | **13** | + | 10 | 36(*S*) |
| **10** | **14** | - | 11 | 14(*S*) |
| **11** | **14** | + | 15 | 14(*S*) |
| **12** | **15** | - | 8 | 5(*S*) |
| **13** | **15** | + | 11 | 18(*S*) |

a) Reaction conditions: acetophenone (1 eq, 0.2 M in 2-propanol), [{$RhCl_2Cp^*$}$_2$] (0.25 mol%), ligand (0.55 mol%) and *i*-PrONa (5 mol%), 2 h at room temperature.

It is a bit more complicated to figure out how the hydroxamic acid part coordinates. By using ligands with different substitution patterns at the hydroxamic acid, the goal was to rule out some possible coordinations.

Using ligand **13**, with a methyl-group on the oxygen, in the reduction of acetophenone, resulted in low conversion (16%) and an *ee* of 70%. When instead ligand **14**, which is methylated at the nitrogen of the hydroxamic acid

function, was employed, an even lower conversion (11%) and low enantioselectivity (14%) was obtained. Having methyl groups on both the oxygen and the nitrogen, **15**, resulted in poor conversion (8%) and an *ee* of 5%. From these results it is apparent that the catalyst gives poor results when the nitrogen in the hydroxamic acid is methylated, whereas methylating only on the oxygen gives a drop in conversion but still decent enantioselectivity. The coordination of the metal in the hydroxamic class of ligands is thus believed to be with the Boc-carbamate nitrogen and the hydroxamic acid function (Figure 6, **B** or **C**). This is consistent with data presented in the literature, where coordination with the nitrogen in the hydroxamic acid and the amine functionalities has been established for an amino acid derived hydroxamic acid under basic conditions.[39b,c]

### 2.3.2 Coordination of the thio amide ligand

With the insight gained from the study of the hydroxamic acids, we next turned our attention towards the coordination of the thio amide ligands.

The result obtained when using the thio amide ligand **16**, made from *S*-(+)-phenyl butyric acid (Table 4), indicates that the Boc carbamate nitrogen plays a crucial role in the binding of rhodium also for this class of ligands. This result rules out the possibility that the thio amide functionality coordinates the metal by itself (Figure 6, **G**). The thio amide catalyst is not as sensitive to variations at the Boc-carbamate nitrogen as the hydroxamic acid or *pseudo*-dipeptide catalysts. Even if catalytic activity is lost when the Boc is replaced with a tosyl group (**17**), both the acetylated ligand, **18**, and the ligand with a primary amine function, **19**, show catalytic activity.

With this knowledge of the importance of substituents at the *N*-terminal, it remains to understand how the thio amide function coordinates to the metal, in order to get the complete picture. In an attempt to do this, ligand **20** was synthesized through methylation of the Boc-protected valine derived thio amide. This ligand has no catalytic activity, showing that the presence of the thio amide proton, which is deprotonated when the catalyst is activated, is crucial. The importance of this proton is further verified by the fact that no conversion is obtained when using ligand **21**.

The alcohol function, which plays a crucial role in the *pseudo*-dipetide ligand system, rather deteriorates the reaction in the case of the thio amide system. A different coordination than in the *pseudo*-dipetide case is therefore probable. The thio amide ligands are thus likely coordinating the rhodium with the Boc-carbamate nitrogen and the sulfur in the thio amide function (**F**, Figure 6).

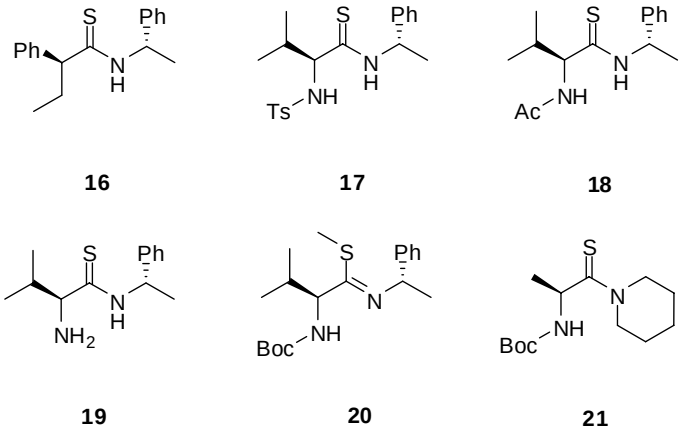


**16** **17** **18**

**19** **20** **21**

**Figure 8.**

**Table 4.** Catalytic results employing ligands **16**-**20**.[a]

| Entry | Ligand | LiCl (5 mol%) | Conversion [%] | *ee* [%] |
|---|---|---|---|---|
| **1** | **16** | - | - | - |
| **2** | **16** | + | 2 | - |
| **3** | **17** | - | 1 | - |
| **4** | **17** | + | 2 | - |
| **5** | **18** | - | 20 | 62(*R*) |
| **6** | **18** | + | 23 | 63(*R*) |
| **7** | **19** | - | 87 | 28(*R*) |
| **8** | **20** | - | - | - |
| **9**[b] | **21** | - | 2 | - |

a) Reaction conditions: acetophenone (1 eq, 0.2 M in 2-propanol), [{$RhCl_2Cp^*$}$_2$] (0.25 mol%), ligand (0.55 mol%) and *i*-PrONa (5 mol%), 2 h at room temperature. b) [{$RuCl_2$(*p*-cymene)}$_2$] (0.5 mol%) was used as metal precursor.

## 2.4 Mechanistic aspects

To get a better understanding of the reasons behind the stereochemical outcome of the reductions, a closer look on the mechanisms is necessary. The reaction between the rhodium-hydride complex and acetophenone most likely proceeds via an outer-sphere bifunctional mono-hydride mechanism (Scheme 2, type III). This implies that the substrate interacts both with the metal hydride and the ligand, and hence the stereochemistry of these two features will influence the outcome of the reaction.

The observed difference in activity of the catalyst upon alteration of the Boc-carbamate function indicates that this is the basic site, serving as a proton acceptor/donor during the reaction. Before the formation of the hydride, the chiral information is present solely in the ligand part of the complex. At this stage, the rhodium is a prochiral, diastereotopic center, and two different hydrides can be formed (Scheme 8). Since the two hydrides are diastereomers they have different energy, and can thus be formed in different ratios.

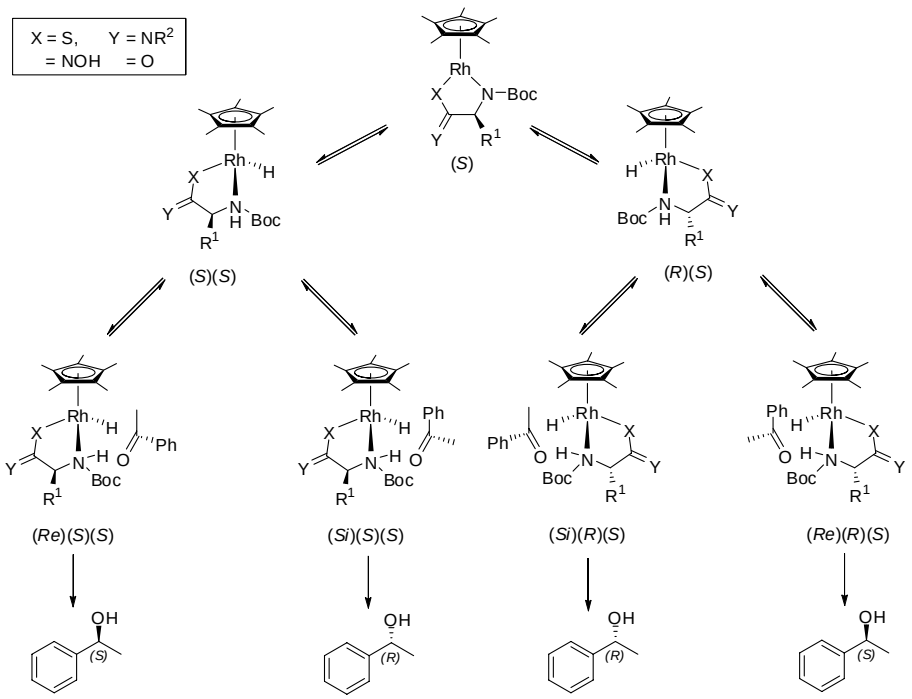


**Scheme 8.** The mechanistic pathways for the asymmetric reduction of acetophenone.

Of these two rhodium-hydride isomers, the (*R*)(*S*)-diastereomer is less sterically crowded and will probably be more stable. This can be seen using a Newman projection through the carbamate nitrogen α-carbon bond (Figure 9). In the (*S*)(*S*)-isomer, the Boc-carbamate group and the substituent of the amino acid, $R^1$, are in a crowded eclipsed conformation. In the (*R*)(*S*)-isomer, the steric interaction between these groups is less pronounced. This trend has also been reported by Wills and co-workers. They observed that a *trans*-relationship of the substituents gave the best activity and selectivity in the ruthenium-mono-tosylated diamine catalyst.[41] When the formation of the hydride is the rate determining step, then the diastereomer with the lowest

[41] Hayes. A.; Clarkson, G.; Wills, M. *Tetrahedron: Asymmetry* 2**004**, *15*, 2079-2084

activation barrier (in this case probably (*R*)(*S*)) will be formed. This is the case for the similar amino-alcohol system.[42]

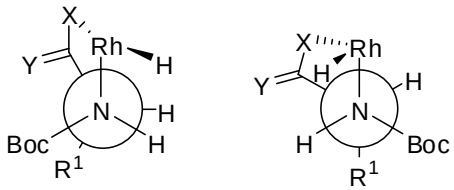


(*S*)(*S*) (*R*)(*S*)

**Figure 9.** Newman-projection through the carbamate nitrogen-carbon bond of the two diastereomers of the rhodium hydride (the cyclopentadienyl ligand is omitted for clarity reasons).

Furthermore, the enantioselectivity is influenced by the manner in which the prochiral ketone interacts with the rhodium-hydride complex. For Noyori's TsDPEN-Ru/Rh catalyst, the stereoselectivity has been ascribed not only to the chiral ligand, but also to the contribution of the arene or cyclopentadienyl ligands on the stabilization of the transition state.[43] The phenyl group can either point away from, or towards the cyclopentadienyl ligand. When pointing away, the transition state is less crowded, however when the phenyl group points towards the cyclopentadienyl ring, arene-substrate C-H/π interactions can further stabilize the transition state. Applied to the thio amide/hydroxamic acid based catalysts, this leads to two different transition states for the hydride transfer for each diastereomer of the catalyst. The (*R*)(*S*) diastereomer of the rhodium-hydride, will thus form the (*S*)-enantiomer of the product alcohol, via the C-H/π stabilized transition state. In order to form the (*R*)-enantiomer, the reaction will have to either proceed without the C-H/π stabilization, or via the sterically unfavourable (*S*)(*S*)-diastereomer of the rhodium-hydride.

If the product formation is the rate determining step, both diastereomers of the hydride will be formed. The product formation will now be controlled by the lowest energy transition state of the four possible paths.
In order to get further information on the reaction mechanisms employing these complexes, a thorough kinetic and theoretical investigation is necessary.

[42] Noyori, R.; Yamakawa, M.; Hashiguchi, S. *J. Org. Chem.* **2001**, *66*, 7931-7944
[43] Yamakawa, M.; Yamada, I.; Noyori, R. *Angew. Chem. Int. Ed.* **2001**, *40*, 2818-2821

## 2.5 Conclusions

By replacing the amide functionality in the *pseudo*-dipeptide ligands with the corresponding thio amide, a switch from the *S*- to the *R*-product is observed when these compounds are used in ATH with rhodium or ruthenium. The use of hydrazides and hydroxamic acids show that it is the presence of the sulfur in the ligand structure rather than higher acidity of the amide proton that is the reason for this switch. Activity studies strongly support that hydroxamic acids coordinate the rhodium via the Boc-nitrogen and the nitrogen in the hydroxamic acid functionality (**B**, Figure 6). The thio amide on the other hand coordinates via sulfur and the Boc-nitrogen (**F**, Figure 6).

We propose that the different coordination modes observed using either thio amide or hydroxamic acid ligands is the reason behind the formation of the products with opposite but high enantioselectivity.

# 3 Fe-Hydrogenase active site model complexes (Paper III)

The Fe-hydrogenases are capable of oxidizing molecular hydrogen to protons and reducing protons to molecular hydrogen under mild conditions. These reactions are believed to proceed via an iron-hydride intermediate. After the X-ray structure of the H-cluster was revealed, model complexes have attracted much interest. Some complexes have been made with the aim of mimicking the structural features of the H-cluster, whereas others have been made with the intent of finding a complex with the properties of the H-cluster, that is, the ability to catalyze proton reduction at mild potentials. The first complexes of the general formula $(\mu\text{-RS})_2Fe_2(CO)_6$ were discovered by Reihlen and co-workers in the first half of the twentieth century (Figure 10).[44] Although not known at the time, the $Fe_2S_2$ cores of these complexes are in a butterfly arrangement, with great resemblance to the di-iron part of the H-cluster. For the synthesis of the di-iron core, a couple of different synthetic protocols have been reported that give access to a number of structural variations in the desired model complexes.

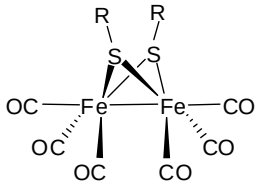


**Figure 10.** Complexes of the general formula $(\mu\text{-RS})_2Fe_2(CO)_6$.

## 3.1 Synthetic methods

The method used by Reihlen for the synthesis of the di-iron-hexacarbonyl complexes was to reflux a thiol with $Fe(CO)_5$. Since then, this protocol has

[44] Reihlen, H.; Gruhl, A.; Hessling, G. *Liebigs. Ann. Chem.* **1929**, *472*, 268-287

been found viable for several different iron(0)carbonyl sources like $Fe_2(CO)_9$ or $Fe_3(CO)_{12,}$ and different chelating dithiolate ligands (Scheme 9a).[45]
Starting from $Fe_2(\mu\text{-}S)_2(CO)_6$, first synthesized by Hieber and Gruber[46] and structurally elucidated by Dahl,[47] there are several alternative routes for synthetic elaboration. The fact that the S-S bond in this complex behaves like an organic disulfide has led to intense studies. If irradiated it adds to alkenes in a [2+2] manner (Scheme 9b).[48] The limitation of this reaction is that the length of the created thiolate bridge is restricted to two carbon atoms.

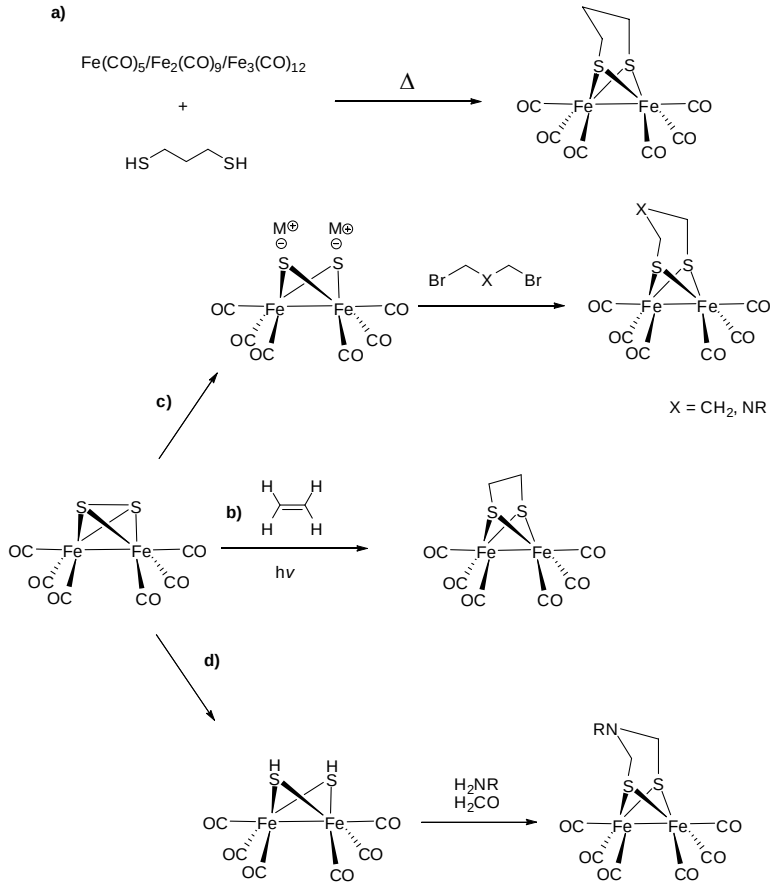


**Scheme 9.** Synthetic methods to obtain complexes of the general formula $(\mu\text{-}(R)S_2)Fe_2(CO)_6$ .

Another synthetic route is to make the Na, Li or K salt of $Fe_2(\mu\text{-}S)_2(CO)_6$ by reacting the latter with sodium metal, superhydride ($LiEt_3BH$) or potassi-

[45] Winter, A. *Naturforsch, B; Anorg. Chem. Org. Chem.* **1982**, *37B*, 1430-1436
[46] Hieber, W.; Gruber, J. Z. *Anorg. Allg. Chem.* **1958**, *296*, 91-103
[47] Wei, C. H.; Dahl, L. F. *Inorg. Chem.* **1965**, *4*, 1-11
[48] Messelhauser, J.; Lorenz, I. -P.; Haug, K.; Hiller, W. *Z. Naturforsch.* **1985**, *40B*, 1064-1067

umhydride. The salt is then reacted with a dihalide (Scheme 9c).[49] Recently a mild method condensing an amine with formaldehyde in the presence of $Fe_2(\mu\text{-}SH)_2(CO)_6$ has been reported as a way of obtaining complexes with the amine in the thiolate bridge (Scheme 9d).[50]

## 3.2 Properties of the model complexes

During the catalytic cycle, the H-cluster uses two protons and two electrons to make molecular hydrogen. Initially, the oxidized form of the H-cluster (Figure 3a) is reduced from the oxidation state $Fe^{II}Fe^{II}$ to $Fe^{II}Fe^{I}$. As the iron ion becomes softer, the bond to the hard ligand L ($H_2O$ or $^-OH$) becomes weaker and the ligand is eventually released. The order in which the subsequent protonations and reductions take place is still unclear.[51] Nevertheless, the H-cluster has properties such that protonations in the peptide environment and reductions at mild potentials are possible.

When trying to mimic the properties of the H-cluster, the reduction potentials and the reactivity of the model complexes towards protons are of immense interest. Studies by Poilblanc and co-workers showed that it is not possible to protonate di-iron hexacarbonyl complexes. However, exchanging one or more carbonyl ligands with more electron-donating phosphines makes the Fe-Fe bond more electron rich and accessible to protonation in an acidic environment.[52] Rauchfuss showed that the amine rather than the Fe-Fe bond is protonated in the $(\mu\text{-adt})Fe_2(CO)_6$ complex in the presence of acid.[53]

The all carbonyl complex with a pdt bridge is reduced at –1.66 V[54] and the complex with an adt bridge at –1.56 V. There are several possible ways to adjust the redox properties of the model complexes. The chelating dithiolate ligand can be changed, different metals can be used or the carbonyls can be replaced with other ligands. Different ligands such as $PPh_3$,[55] $PMe_3$,[56] $PMe_2Ph$, $P(OR)_3$,[57] $CN^-$,[58] CNR[59] and carbenes[60] have been introduced. The

[49] a) Seyferth, D.; Song, L. -C.; Henderson, R. S. *J. Am. Chem. Soc.* **1981**, *103*, 5103-5107; b) Song, L. -C. *Acc. Chem. Res.* **2005**, *38*, 21-28
[50] Li, H.; Rauchfuss, T. B. *J. Am. Chem. Soc.* **2002**, *124*, 726-727
[51] a) Armstrong, F. A. *Curr. Opin. Chem. Biol.* **2004**, *8*, 133-140; b) De Lacey, A. L.; Fernández, V. M.; Rousset, M.; Cammack, R. *Chem. Rev.* **2007**, *107*, 4304-4330
[52] a) Fauvel, K.; Mathieu, R.; Poilblanc, R. *Inorg. Chem.* **1976**, *15*, 976-978; b) Arabi, M.S., Mathieu, R.; Poilblanc, R. *J. Organomet. Chem.* **1976**, *177*, 199-209
[53] Lawrence, J. D.; Li, H.; Rauchfuss, T. B.; Bénard, M.; Rohmer, M. M. *Angew. Chem. Int. Ed.* **2001**, *40*, 9, 1768-1771
[54] All potentials are given vs $Fc^+/Fc$ ($Fc^+/Fc$ is 0.37 V vs SCE)
[55] Hasan, M. M.; Hursthouse, M. B; Kabir, S. E.; Malik, K. M. A. *Polyhedron* **2001**, 97-101
[56] Zhao, X.; Georgakaki, I. P.; Miller, M. L.; Meija-Rodriguez, R.; Chiang, C. -Y.; Darensbourg, M. Y. *Inorg. Chem.* **2002**, *41*, 3917-3928
[57] Li, P.; Wang, M.; He, C.; Li, G.; Liu, X.; Chen, C.; Åkermark, B.; Sun, L. *Eur. J. Inorg. Chem.* **2005**, 2506-2513

smaller ligands readily undergo disubstitution whereas more sterically hindered ligands generally displace only one CO. The bis-cyanide complex is reduced at –2.7 V[58b] and the mono $PPh_3$ substituted complex is reduced at –1.84 V.

More electron donating ligands such as phosphines initially have an unfavourable effect as the reduction potentials of these complexes are even more negative. However, the complexes become more basic, and once protonated at the Fe-Fe bond, the reduction potential shifts to more positive values, thereby overcompensating for the unfavourable initial effect of the electron donating ligand (Scheme 10).[61]

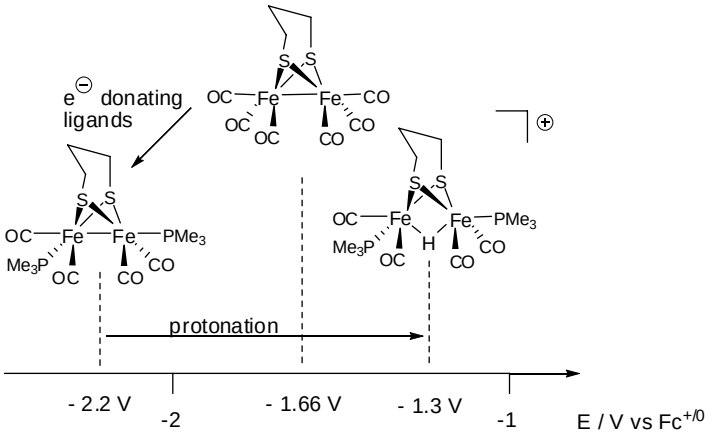


**Scheme 10.** Introducion of electron donating ligands that enable subsequent protonation and their effect on the reduction potential of the complexes.

Darensbourg and co-workers noticed that (μ-pdt)$Fe_2(CO)_4(PMe_3)_2$ scrambles $H_2/D_2$ in acidic environment.[62] Rauchfuss and co-workers have performed electrochemical $H_2$ production using (μ-pdt)$Fe_2(CO)_4(CN)(PMe_3)^-$ at a potential of –1.56 V[61a] and Ott et. al have achieved electrochemical $H_2$ production using (μ-adt)$Fe_2(CO)_6$ at a potential of –1.4 V.[63] The proposed mechanisms for the reactions of these two complexes differ. Rauchfuss has

[58] a) Schmidt, M.; Contakes, S. M.; Rauchfuss, T. B. *J. Am. Chem. Soc.* **1999**, *121*, 9736-9737 b) Le Cloire, A.; Best, S. P.; Borg, S.; Davies, S. C.; Evans, D. J.; Hughes, D. L.; Pickett, C. J. *Chem. Commun.* **1999**, 2285-2286 c) Lyon, E. J.; Georgakaki, S. M.; Riebenspeis, J. H.; Darensbourg, M. Y. *Angew. Chem. Int. Ed.* **1999**, *38*, 21, 3178-3180

[59] Nehring, J. L.; Heinekey, D. M. *Inorg. Chem.* **2003**, *42*, 4288-4292

[60] Capon, J. -F.; Hassnaoui, S. E.; Gloaguen, F.; Schollhammer, P.; Talarmin, J. *Organometallics* **2005**, *24*, 2020-2022

[61] a) Gloaguen, F.; Lawrence, J. D.; Rauchfuss, T. B. *J. Am. Chem. Soc.* **2001**, *123*, 9476-9477; b) Gloaguen, F.; Lawrence, J. D.; Rauchfuss, T. B.; Bénard, M.; Rohmer, M. -M. *Inorg. Chem.* **2002**, *41*, 6573-6582

[62] Zhao, X.; Georgakaki, I. P; Miller, M. L.; Yarbrough, J. C.; Darensbourg, M. Y. *J. Am. Chem. Soc.* **2001**, *123*, 9710-9711

[63] Ott, S.; Kritikos, M.; Åkermark, B.; Sun, L.; Lomoth, R. *Angew. Chem. Int. Ed.* **2004**, *43*, 1006-1009

suggested a CCEE (chemical-chemical-electrochemical-electrochemical) sequence of events, whereas Ott has suggested a CECE mechanism for his complex. In the catalytic cycle of the enzyme the oxidation states for the iron centers vary between +2 and +1, and for some model complexes they vary between +2 and +1,[61a] whereas the oxidation states for other model complexes varies between +1 and 0. So, it is apparent that the mimics don't need to have the exact features of the H-cluster in order to show catalytic activity, and that differences in the mimics causes the proton reduction to proceed by different mechanisms.

## 3.3 Dynamic Ligation at the first amine coordinated hydrogenase active site mimic

An interesting feature in the reported crystal structure of the H-cluster is the carbonyl ligand that occupies a bridging position between the two iron ions. In combination with the loosely bound ligand ($^{-}$OH or $H_2O$) at the distal iron, this bridging carbonyl gives the distal iron in the H-cluster a dynamic ligation sphere. Upon the initial reduction, the ligand dissociates, making the complex coordinatively unsaturated with a free coordination site where chemistry can occur. The model complexes synthesized by Reihlen among others do not contain the bridging carbonyl and are ligated by soft ligands such as CO, $CN^{-}$, $PR_3$ and $RS^{-}$. Complexes with hard ligands such as alcohols, alkoxides and amines have not been studied as extensively, mostly due to the fact that they are labile and hard to isolate.

## 3.4 Synthesis and structure

Rauchfuss and co-workers reported the synthesis of di-iron complexes containing a bridging CO.[64] The complex is oxidized from $Fe^{I}Fe^{I}$ to $Fe^{II}Fe^{II}$ in the presence of a phosphine, cyanide or methyl *iso*-cyanide ligand. The result is a complex containing a bridging carbonyl, but these complexes instead lack a free coordination site around the irons.

Primary amines have been used as decarbonylation reagent for iron hydrogenase model complexes, thereby making ligand substitution possible. When (μ-pdt)$Fe_2(CO)_6$ was refluxed in *n*-propylamine for a few hours, TLC analysis showed complete consumption of starting material and appearance of a new complex. This complex was stable in non-coordinating solvents such as pentane and toluene. In the absence of an additional ligand, the free

[64] a) Boyke, C. A.; Rauchfuss, T. B.; Wilson, S. R.; Rohmer, M. -M.; Bénard, M. *J. Am. Chem. Soc.* **2004**, 126, 15151-15160; b) Boyke, C. A.; van der Vlugt, J. I; Rauchfuss, T. B; Wilson, S. R.; Zampella, G.; De Giola, L. *J. Am. Chem. Soc.* **2005**, *127*, 11010-11018

coordination site available after the decarbonylation is instead occupied by the solvent amine and the complex (μ-pdt)$Fe_2(CO)_5(H_2NPr)$ **19** was isolated in 48% yield after purification (Scheme 11).

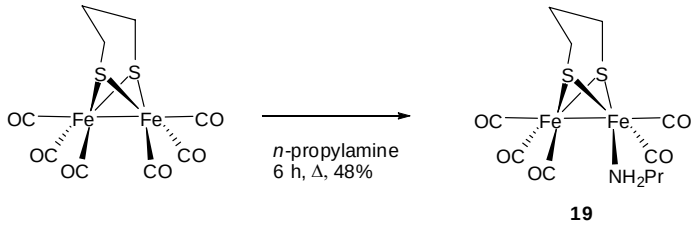


**19**

**Scheme 11.**

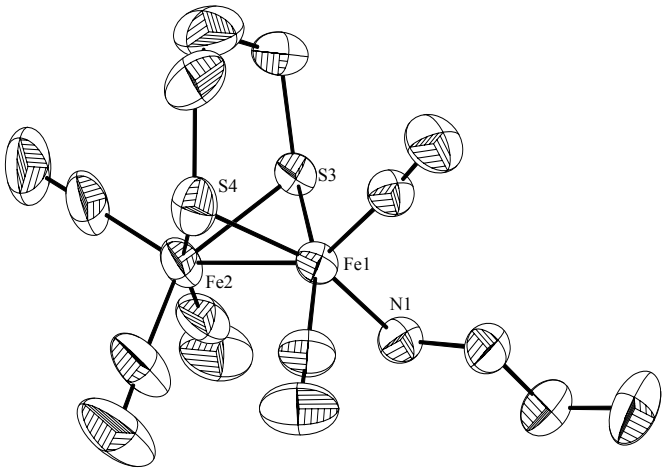


**Figure 11.** The crystal structure of **19**.

The structure of **19** was confirmed by single crystal X-ray analysis (Figure 11), which shows that the *n*-propylamine ligand coordinates one of the iron ions in a basal position. From the structure it can also be seen that the Fe-Fe bond distance of **19** is 2.55 Å, slightly longer than that of the hexacarbonyl complex (2.51 Å). The distance between the iron and the nitrogen of the propylamine ligand is 2.07 Å. This bond is shorter than the Fe-P bond in complexes with phosphines (usually around 2.2 Å), most likely due to the smaller nature of the nitrogen as compared to the phosphorous.

Although the *n*-propylamine is not in an apical position as is the loosely bound ligand in the H-cluster, the introduction of an easily removable ligand in the coordination sphere of the iron ion has been achieved.

## 3.5 Reactivity and properties

Complex **19** is stable in non coordinating solvents and the IR spectrum of the complex remains unchanged over time. In the coordinating solvent $CH_3CN$ however, **19** is consumed and a new complex **20** is formed. From the IR spectra it can be concluded that **20** is similar in structure to **19**, as a similar pattern is noted, though somewhat shifted towards higher energy (see Figure 12).

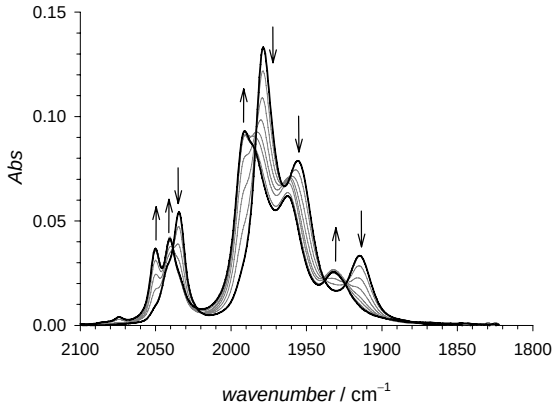


**Figure 12.** The spectral changes in the carbonyl region of the IR spectrum upon the transformation from **19** to **20**.

This observation can be explained by the substitution of the amine ligand by a solvent molecule. The explanation is further supported by the fact that addition of excess *n*-propylamine to **20** regenerates **19** (as can be seen by IR). Thus there seems to be an equilibrium between **19** and **20**. In MeCN, this equilibrium is strongly shifted towards **20**, but the addition of *n*-propylamine reverses it to **19**.

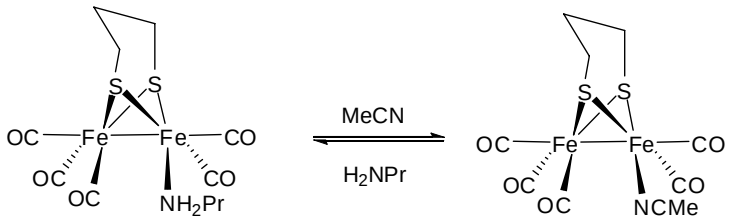


**19** **20**

**Scheme 12.** The equilibrium between **19** and **20**.

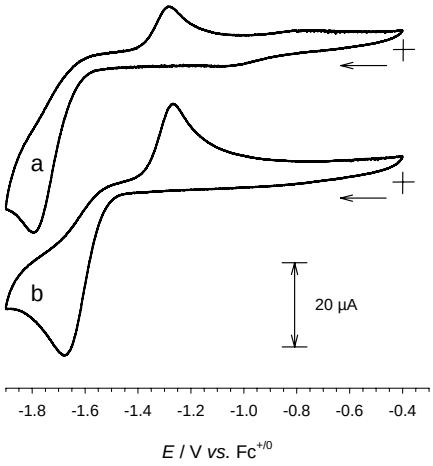


**Figure 13.** The cyclovoltammogram (100 mV/s) of: a) **19** obtained in the presence of excess *n*-propylamine and b) **20** in MeCN solution.

The cyclic voltammogram of **19**, Figure 13, features a reduction E = –1.80 V, whereas the reduction is shifted to E = –1.68 V for **20**. The shift is due to stronger electron donor ability of the *n*-propylamine. The re-oxidation for **19** and **20** occurs at the same potential, E = –1.28 V, indicating that the reduction of these complexes leads to the same reduced species $\mathbf{21}^{-}$. This theory is further confirmed by FTIR-spectroelectrochemistry. The spectrum before and after the reduction of **19** at –1.80 V and **20** at –1.68 V respectively, are shown in Figure 14. From these spectra it is apparent that the same specie $\mathbf{21}^{-}$ is formed in both cases.

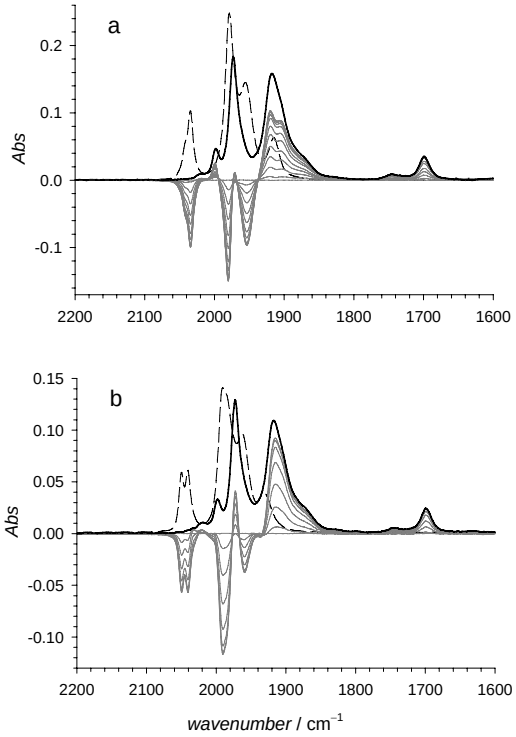


**Figure 14.** IR spectrum of complex **19** (a) and **20** (b) before (dashed line) and after (solid line) the electrochemical reduction at –1.98 and –1.78 V, respectively. Grey traces are difference spectra recorded during the course of the electrolysis.

The number of ligands cannot be determined from these data, however it is reasonable to assume that after the reduction the complex looses the labile ligand ($CH_3CN$ or *n*-propylamine) in order to stabilize the negative charge on the metal. The re-oxidation of $\mathbf{21}^-$ leads to an intermediate, **21**, which again coordinates the respective ligand $CH_3CN$ or *n*-propylamine. From these results a cycle for the transformations of **19** was proposed (Scheme 13). Both **19** and **20** are 18-electron complexes with respect to both iron ions. After the initial reduction, one of the irons instead acquires a 19-electron configuration. By expelling the labile ligand, the complex turn into a 17-electron complex, which thus is somewhat stabilized. This is in analogy with the activation of the catalytically inactive, fully oxidized state of the H-cluster. Recently, Pickett and Best were able to isolate a species, obtained from the reduction of a complex similar to **19**, in solid form.[65] It turned out that the complex had dimerized in order to form a more stabilized 18-electron complex.

[65] Best, S. P.; Borg, S. J.; White, J. M.; Razavet, M.; Pickett, C. J. *Chem. Commun.* **2007**, 4348-4350

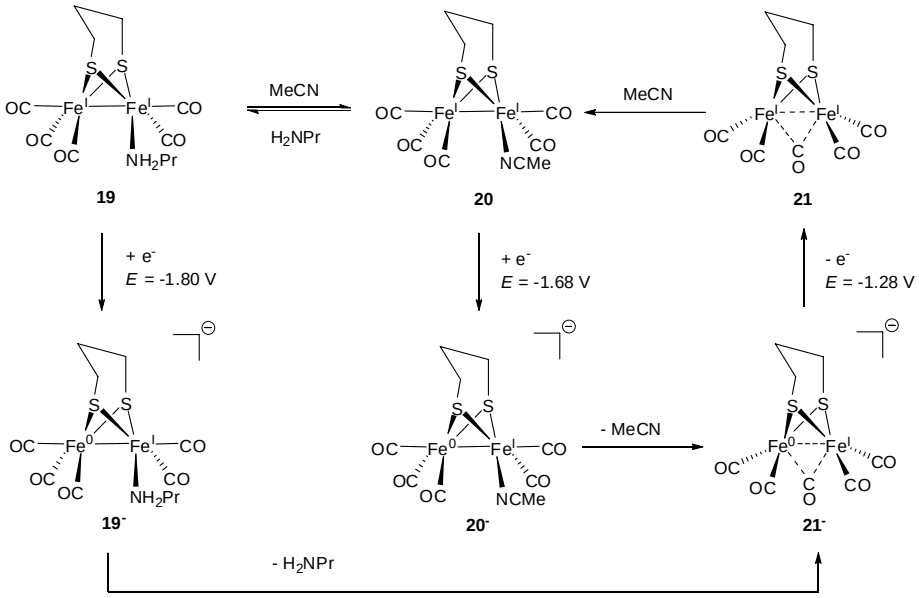


**Scheme 13.** A proposed cycle for the electrochemical transformations of complex **19**.

## 3.6 Conclusions

There are many intriguing features, including the loosely bound ligand and the bridging carbonyl, in the H-cluster. Together they make the enzyme an efficient environment for the reduction of protons at mild potentials. Much research has focused on the nitrogen in the dithiolate bridge and on the introduction of various soft ligands and their functions. The loosely bound ligand on the distal iron has been studied much less. With the synthesis of **19**, a di-iron complex with a labile ligand has been realised. This ligand can easily be displaced by coordination of a solvent molecule, and upon reduction the ligand dissociates. These properties make the complex a possible synthon for a di-iron complex with a free coordination site, and a bridging carbonyl.

# 4 Towards light induced hydrogen production (Paper IV)

In order to complete a catalytic cycle and reduce protons to molecular hydrogen, the active site of the hydrogenase needs two electrons. Different proteins such as cythochrome $c_3$ and cythochrome $c_6$ act as electron donors (or acceptors for the reverse reaction) and deliver the electrons to the hydrogenase.[66] These electrons are transported to the H-cluster via the $Fe_4S_4$-cube. Iron-sulfur cubic complexes function as redox relays and are part of electron transport chains in many protein systems.[67]

In some green algae, the hydrogenase obtains electrons for the proton reduction from the photosynthetic light reaction.[68] The hydrogen production in these organisms is thus light induced. In the same manner Amao et. al have shown that by coupling a hydrogenase from *Desulfovibrio vulgaris* to viologen-linked porphyrins, light induced $H_2$ production can be achieved.[69] Our desire is to use this concept: to get access to electrons from a photosensitizer, but instead of a protein, using a model complex as the catalytic center.[70]

## 4.1 Properties of the photosensitizer

The photosensitizer should have the ability to absorb a photon and from the excited state eject an electron to an acceptor. In photosynthesis, the photosensitizer consists of a pair of porphyrins. Porphyrins have also been used as photosensitizers in synthetically made systems.[71] Other complexes often used as photosensitizers are ruthenium polypyridyls such as ruthenium trisbipyridine or ruthenium bistripyridine. Ruthenium trisbipyridine has many desirable properties. It absorbs light in the visible region, has a long excited state lifetime, good redox potentials for both oxidation and reduction in the excited state, is chemically robust and is easy to functionalize.

---

[66] Vignais, P. M.; Billoud, B.; Meyer, J. *Microbiol. Rev.* **2001**, *25*, 455-501
[67] Venkateswara, P.; Holm, R. H. *Chem. Rev.* **2004** *104*, 2, 527-559
[68] Greenbaum, E.; Blankinship, S. L.; Lee, J. W.; Ford, R. M. *J. Phys. Chem. B.* **2001**, *105*, 3605-3609
[69] Amao, Y.; Kamachi, T.; Okura, I. *J. Porphyrins. Phtalocyanines* **1998**, *2*, 201-207
[70] Sun, L.; Åkermark, B.; Ott, S. *Coord. Chem. Rev.* **2005** *249*, 1653-1663
[71] Wasielewski, M. R. *Chem. Rev.* **1992**, *93*, 435-461

The absorption of $[Ru(bpy)_3]^{2+}$ at 452 nm has been assigned to a metal-to-ligand charge transfer ($^1$MLCT) of an electron in the dπ of the metal to the $\pi^*$ of the ligand.[72] This state rapidly decays to the triplet state ($^3$MLCT). This is the state from which electron transfer processes are observed.

## 4.2 Hydrogenase model complexes coupled to photosensitizers

Some examples of hydrogenase model complexes coupled to different photosensitizers have been reported in the literature. Song and co-workers have coupled a hydrogenase model complex to a porphyrin.[73] Whether electron transfer from the photosensitizer to the Fe-moiety can occur depends on if the excited state of the sensitizer has a sufficiently long lifetime and if there is a beneficial driving force for this process. The driving force for electron transfer from the photosensitizer to the iron part can be calculated from the excited state energy, $E^{00}$, and oxidation potential of the photosensitizer, $E^0(P^{+/0})$, together with the reduction potential of the di-iron acceptor, $E^0(A^{0/-})$, using the Rehm-Weller equation:[74]

$$\Delta G = E^0\left(P^{+/0}\right) - E^0\left(A^{0/-}\right) - E^{00}$$

With an oxidation potential in the excited state of –0.64 V for the porphyrin and a reduction potential of –1.56 V for the adt hexacarbonyl iron-acceptor part, a driving force of ΔG = 0.92 V can be calculated. This means that the driving force is not sufficient for electron transfer from the porphyrin to the hydrogenase model part. Recently Song and co-workers have reported a second complex, with an adt-hydrogenase model complex coordinated to a Zn-porphyrin. Even though this complex has somewhat more suitable properties, it has an oxidation potential of –1.04 V in the excited state;[72] it is still not sufficient for electron transfer to the iron-acceptor.

A model complex with a free amine functional group has been synthesized by Salyi et. al[75] and coupled to a ruthenium trisbipyridine photosensitizer by Wolpher et. al.[76] The excited state of this dyad decays by a double exponential function with two excited state lifetimes, $\tau_1$ = 234 ns and $\tau_2$ =

---

[72] Kalyanasundaram, K. *Photochemistry of Polypyridine and Porphyrin Complexes,* Academic Press Limited, London **1992**, 87-212
[73] Song, L. *Angew. Chem.* **2006**, *45*, 1130-1133
[74] a) Rehm, D.; Weller, A. *Isr. J. Chem.* **1970**, *8*, 259-271; b) Weller, A. *Zeitschrift fuer Physikalische Chemie* **1982**, *133*, 93-98
[75] Salyi, S.; Kritikos, M.; Åkermark, B.; Sun, L. *Chem. Eur. J.* **2003**, *9*, 557-560
[76] Wolpher, H.; Borgström, M.; Hammarström, L.; Bergquist, J.; Sundström, V.; Styring, S.; Sun, L.; Åkermark, B. *Inorg. Chem. Commun.* **2003**, *6*, 989-991

1190 ns. The behavior of the decay is explained by the ability of the flexible linker to bend in space. Compared to an amide functionalized $[Ru(bpy)_3]^{2+}$ reference complex, the dyad is quenched to 70%. Due to its redox properties, the iron moiety is reduced at –1.6 V, the electron transfer from ruthenium to the di-iron site is endothermic by 0.4 V. Since the driving force for electron transfer is unfavourable, the quenching is due to energy transfer. Another model complex, where the di-iron unit is linked to a $Ru(tpy)_2$ part through a rigid acetylene has been synthesized by Ott et. al.[77] The excited state lifetime of this complex is a mere 6.5 ns (because of the generally shorter lifetimes of the $[Ru(tpy)_2]^{2+}$ complexes compared to the $[Ru(bpy)_3]^{2+}$,[72]).

This complex is quenched to 50%. As is the case with the hexacarbonyl complexes, this complex has an unfavourable driving force so energy transfer is the reason for the quenching.

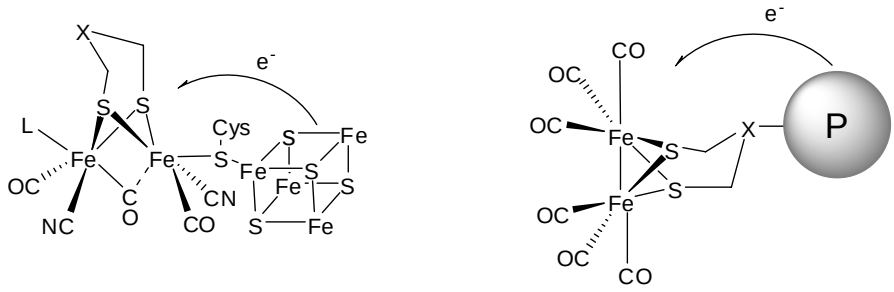


**Figure 15.** Electron transfer in the H-cluster and the model complexes from the literature.

## 4.3 Biomimetic coupling of a hydrogenase model complex to a photosensitizer

The previously synthesized hydrogenase model complexes which were linked to porphyrin or ruthenium polypyridyl photosensitizers had the common feature that they were attached to each other at the central position of the thiolate bridge (Figure 15). In the enzyme however, the di-iron part of the H-cluster is attached to the iron-sulfur cubane at the proximal iron. Therefore the aim was to couple the hydrogenase model to the photosensitizer in a more biomimetic fashion; through a ligand.

In the design of the target molecule **22** (Figure 16), several functional and synthetic aspects were taken into consideration. A triphenylphosphine ligand was chosen as the connection between the ruthenium and the di-iron moiety

[77] Ott, S.; Borgström, M.; Kritikos, M.; Lomoth, R.; Bergquist, J.; Åkermark, B.; Hammarström, L.; Sun, L. *Inorg. Chem.* **2004**, *43*, 15, 4683-4692

because it is relatively easy to functionalize, it forms stable monosubstituted complexes with di-iron hexacarbonyl complexes and it is more stable towards oxidative degradation than trialkylphosphines.

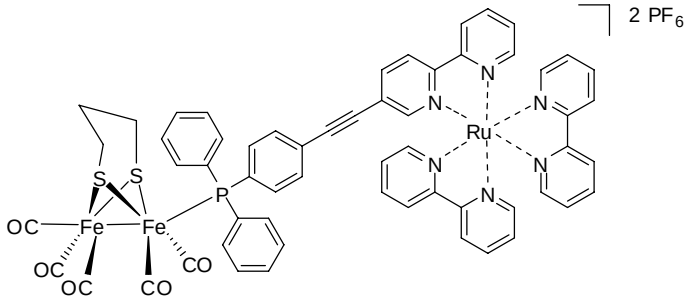


**22**

**Figure 16.** The target molecule.

An acetylene was chosen as the linker due to its linear geometry and rigidity. Finally, $Ru(bpy)_3$ was chosen as photosensitizer because it has a long excited state lifetime combined with high excited state energy.

## 4.4 Synthesis and structure

The di-iron precursor $(\mu\text{-pdt})Fe_2(CO)_6$, was synthesized by refluxing $Fe_3(CO)_{12}$ and 1,3-propanedithiol in THF. A functionalized phosphine, diphenyl(*p*-bromophenyl)phosphine, **23**, was synthesized by reacting 1,4-dibromobenzene with *n*-BuLi and chlorodiphenylphosphine. The obtained phosphine **23** was coordinated to the di-iron complex using $Me_3NO$ as decarbonylation reagent at room temperature to form **24** in 55% yield (Scheme 14). Increasing the amount of $Me_3NO$ results in further ligand exchange to the disubstituted complex, **25**. The $Fe_2S_2$-core of this complex is in the butterfly arrangement (Figure 17). Because of the sterical interference the phosphine ligands seems to prefer apical apical positions. This is not the case in the complex with sterically less hindered phosphines.

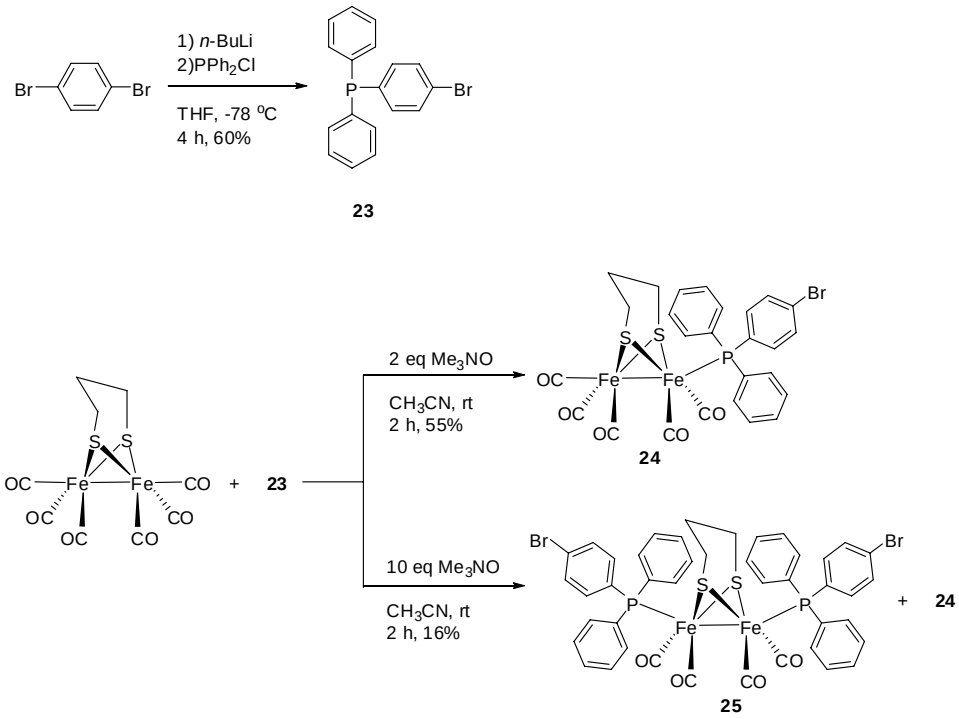


**Scheme 14.**

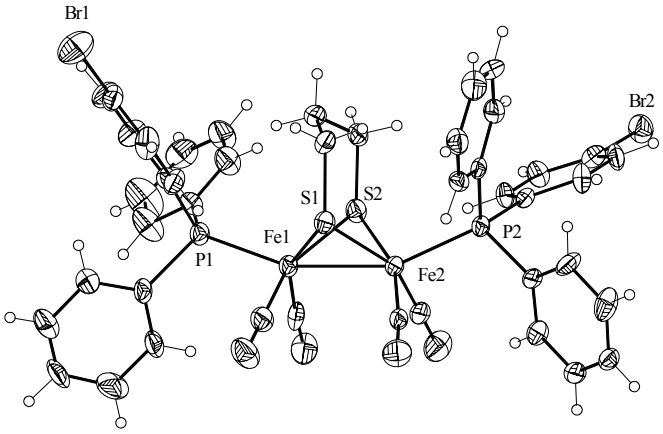


**Figure 17.** Crystal structure of complex **25**.

Unfortunately, no product was isolated when reacting the iron-complex **24** with a terminal acetylene in a Sonogashira coupling reaction[78] (neither microwave nor conventional heating produced any product). The reaction performed on the free ligand **23** did not result in the formation of any product either. So it seems that the bromo-aryl group is too unreactive in the initial oxidative addition step in the coupling reaction.

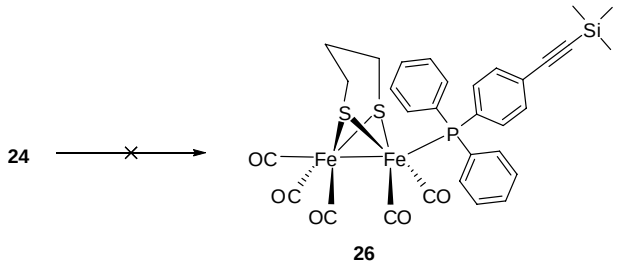


**26**

**Scheme 15.**

Since the introduction of the acetylene to **24** failed, a different approach was used. Instead of making the functionalized phosphine substituted complex prior to the reaction with the acetylene, the acetylene was introduced in the first step. By reacting 1-bromo-4-iodobenzene under Sonogashira conditions with trimethylsilylacetylene, 1-bromo-4-trimethylsilylacetylenebenzene **27**, was obtained in 72% yield (Scheme 16). Next, **27** was lithiated in the bromo position, reacted with chlorodiphenylphosphine and coordinated to (μ-pdt)$Fe_2(CO)_6$, giving **26** in 47% overall yield. As decarbonylation reagent, *n*-propylamine was used. In line with previously reported crystal structures of triphenylphosphine substituted complexes, the phosphine is in the apical position. The Fe-Fe bond is 2.52 Å, with the usual butterfly arrangement of the $Fe_2S_2$ unit (Figure 18).

The TMS group was removed in good yield by stirring complex **26** in a solution of $K_2CO_3$ in THF/MeOH.

[78] Sonogashira, K.; Tohda, Y.; Hagihara, N. *Tetrahedron Lett.* **2005**, *50*, 4467-4470

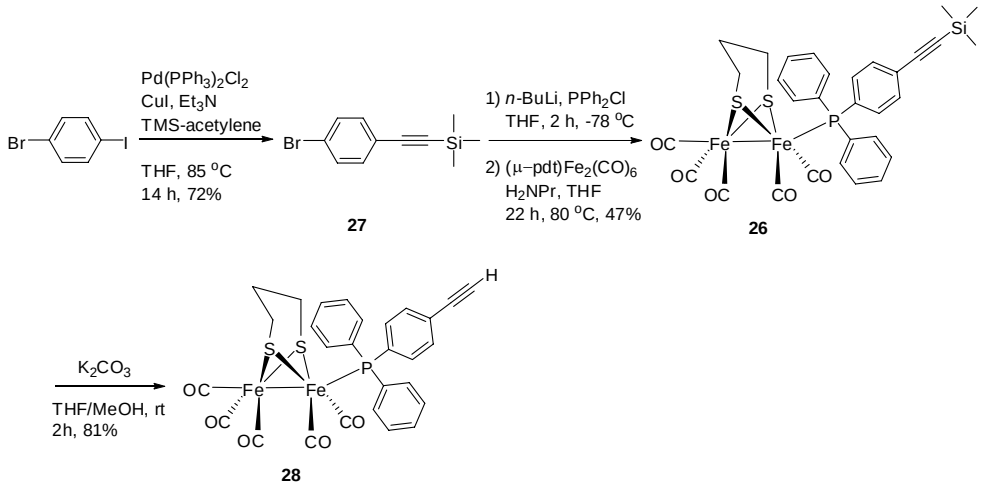


**Scheme 16.**

The reaction of **28** with 5-bromo-2,2´-bipyridine,[79] under Sonogashira conditions, did not result in the formation of any product. It has been noticed before that the iron moiety is not stable in the presence of free polypyridyls.[80] Taking this into consideration, complex **28** was reacted with the fully assembled $[Ru(bpy)_2(5\text{-bpy-Br})]^{2+}$ instead. Using standard Sonogashira conditions, the target molecule **22** was formed in 59% yield. The ESI mass spectrum of **22** shows the typical isotopic pattern for ruthenium complexes at 1357.11 (corresponding to the charged complex resulting from the loss of a $PF_6^-$). The NMR spectra and the elemental analysis further confirm the assigned structure.

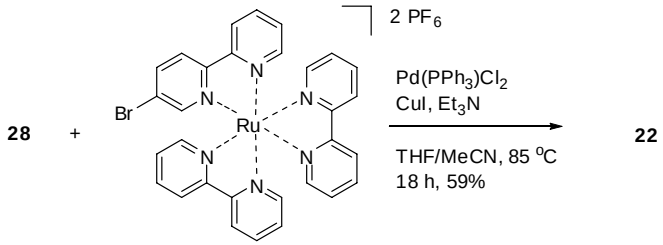


**Scheme 17.**

[79] Romero, F. M.; Ziessel, R. *Tetrahedron Lett.* **1995**, *36*, 6471-6474
[80] Ott, S.; Kritikos, M.; Åkermark, B.; Sun, L. *Angew. Chem. Int. Ed.* **2003**, *42*, 3285-3288

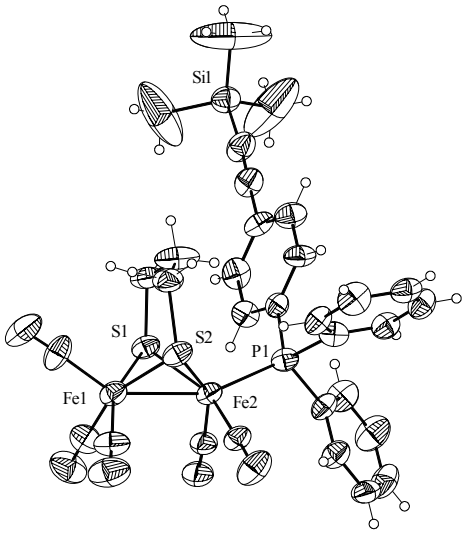


**Figure 18.** Crystal structure of complex **26**.

## 4.5 Electrochemistry

As expected, the monosubstituted complexes **24**, **26** and **28** have electrochemical reductions around –1.7 V and oxidations around 0.4 V. This is a shift to more negative potentials compared to the hexacarbonyl complex, which can be explained by the more electron donating properties of the introduced phosphines. Due to the influence of yet another electron donating ligand in the disubstituted complex **25**, the irreversible oxidation is shifted by 300 mV and the reduction by 150 mV to more negative potentials. As with all the other monophosphine-substituted complexes, dyad **22** has an irreversible reduction associated with the di-iron portion at –1.76 V. The dyad also features a reduction at –1.51 V. The reversible nature of this reduction and a comparison with the reduction of a related complex $[(bpy)_2Ru(5\text{-}bpy\text{–}{\equiv}\text{–}Ar)]^{2+}$,[81] shows that this process corresponds to the reduction of the acetylenic extended bipyridine ligand. A third reduction can be observed at –2.01 V for dyad **22** which is assigned to the reduction of an auxiliary bipyridine ligand.

Because the ligand with the most positive reduction potential is usually the ligand that is involved in the MLCT state, it appears that the MLCT is directed towards the di-iron portion in **22**.

[81] Chaignon, F.; Torroba, J.; Blart, E.; Borgström, M.; Hammarstöm, L.; Odobel, F. *New. J. Chem.* **2005**, *29*, 1272-1284

## 4.6 Photophysics

Low temperature emission measurements at 77 K show that the excited state energy, $E^{00}$, of **22** is 2.01 eV. This value is lower than that of $[Ru(bpy)_3]^{2+}$ (2.13 eV). The decrease is probably due to the conjugation of the acetylene in the linking bpy of **22**. This is supported by the fact that the reference complex $[(bpy)_2Ru(5\text{-}bpy{-}{\equiv}{-}Ar)]^{2+}$ has an $E^{00}$ of 2.04 eV, similar to that of **22**.

The measured excited state lifetime of **22** is 770 ns at room temperature. The reference complex, $[(bpy)_2Ru(5\text{-}bpy{-}{\equiv}{-}Ar)]^{2+}$ has a lifetime of 1200 ns. A comparison shows that the excited state of **22** is quenched to 35% by either electron or energy transfer.

The quantum yield (the amount of the excited state that decays in a radiative way) for complex **22** is 6% of that for the reference complex. So the emission quenching for the complex is substantial. Using the Rehm-Weller equation, the driving force for electron transfer from the excited state of the ruthenium chromophore to the di-iron unit was calculated to be uphill by 0.66 V. Since the absorption and emission spectra do not overlap, energy transfer is not likely to occur. Instead a positive driving force of 100 mV can be calculated for the reductive quenching of the excited state by the di-iron unit. This means that the electrons actually are transferred from the di-iron unit to the ruthenium chromophore.

The photophysical properties of **22** change when the complex is exposed to light. Recording one single emission spectra of **22** or exposure of a solution of **22** to room light for less than one minute leads to significant changes. This behavior is probably due to light-induced oxidative decomposition of the di-iron portion of **22**.

## 4.7 Conclusions

A new strategy has been realized with the synthesis of dyad **22**, in which a model of the iron hydrogenase active site has been coupled to a photosensitizer directly via a ligand. Because the linking acetylenic bipyridine is the most easily reduced ligand, it can be concluded that the excited state is localized towards the di-iron unit. Since the goal is to get electron transfer to the di-iron unit, this is a desirable feature. Due to the redox properties of the di-iron unit the electrons have a positive driving force for going in the opposite direction. Inclusion of an amine in the dithiolate-bridge or further ligand substitution would enable protonation of the di-iron unit and thus render a subsequent reduction more facile. Another way to affect the direction of the electron transfer would be to adjust the oxidation potential of the photosensitizer. This can be achieved either by changing the ligand sphere around the

Ru-center,[82] or by doing an initial reduction of the excited state.[83] A drawback with dyad **22** is its light sensitivity and that it decomposes upon radiation to some extent.

[82] Abrahamsson, M.; Jäger, M.; Österman, T.; Eriksson, L.; Persson, P.; Becker H. -C.; Johansson, O.; Hammarström, L. *J. Am. Chem. Soc.* **2006**, *128*, 12616-12617
[83] Na, Y.; Pan, J.; Wang, M.; Sun, L. *Inorg. Chem.* **2007**, *46*, 3813-3815

# 5. Transfer hydrogenation catalyzed by environmentally friendly catalysts (Paper V)

The reduction of ketones to secondary alcohols is normally performed using catalysts based on transition metals such as Rh, Ru and Ir. The disadvantage with the use of these metals is that they are expensive and not very environmentally benign. For instance, when applied in the synthesis of pharmaceuticals, much effort has to be made in the purification of the products in order to remove the remainings of the catalyst. A significantly better approach would be to use a cheaper and less toxic metal source. In the literature, few procedures using other metals are reported. Relatively few examples of Fe-catalyzed reductions have been reported and among these, hydrogenation of double bonds is mainly described.[84] Nevertheless, there are some examples of Fe-catalyzed transfer hydrogenation presented in the literature. Casey and Guan[85] have published the transfer hydrogenation of aryl alkyl ketones in 2-PrOH using Knölker's complex,[86] an analogue of the Shvo complex (Figure 19).[87] Beller and co-workers have published a procedure for the transfer hydrogenation of ketones using different iron sources in combination with various ligands and base as catalyst.[88]

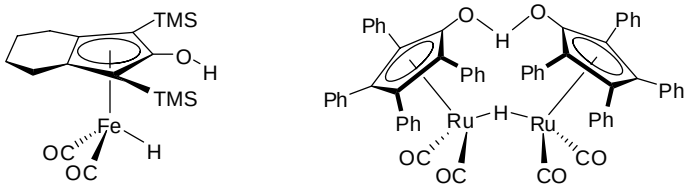


**Figure 19.** The Knölker and the Shvo complex.

[84] a) Bart, S. C.; Lobkovsky, P. J.; Shikrik, P. J. *J. Am. Chem. Soc.* **2004**, *126*, 13794-13807; b) Bart, S. C.; Hawrelak, E. J.; Lobkovsky, P. J.; Shikrik, P. J. *Organometallics* **2005**, *24*, 5518-5527

[85] Casey, C. P.; Guan, H. *J. Am. Chem. Soc.* **2007** *129*, 5816-5817

[86] Knölker, H. -J.; Baum, E.; Goesmann, H.; Klauss, R. *Angew. Chem. Int. Ed.* **1999**, *38*, 2064-2066

[87] Blum, Y.; Czarkle, D.; Rahamim, Y.; Shvo, Y. *Organometallics* **1985**, 1459-1461

[88] a) Enthaler, S.; Hagemann, B.; Erre, G.; Junge, K.; Beller, M. *Chem. Asian. J.* **2006**, *1*, 598-604; b) Enthaler, S.; Erre, G.; Kin Tse, M.; Junge, K.; Beller, M. *Tetrahedron Lett.* **2006**, 8095-8099

## 5.1 Alkali alkoxide catalyzed transfer hydrogenation

The goal was to develop an Fe-based catalyst that is able to efficiently catalyze the reduction of ketones under hydrogen transfer conditions. We found that heating a 2-PrOH solution of acetophenone in the presence of $FeCl_2$, triphenylphosphine and base resulted in the conversion to the corresponding alcohol. This result is in line with results later published by Beller and coworkers.[88] To our surprise, we found that the same results were obtained when excluding the iron source and simply performing the reaction in the presence of the alkali base. This result indicates that the alkali base itself catalyzes the product formation. Alkali alkoxide mediated transfer hydrogenation has been reported earlier, however due to the low activity associated with the alkali alkoxides these reactions require stoichiometric amounts of base.[89] MVPO-like reactions without any catalyst or mediator, performed at temperatures over 300 °C, have also previously been reported.[90]

As a consequence of the finding above, we made a set of experiments in which we screened different alkali bases by heating a 2-propanol solution of actophenone in a sealed pyrex tube at 120 °C for 90 minutes, using microwave irradiation for fast and efficient heating. With a 2-propanol solution of potassium hydroxide (6 mol%), a conversion of 15% to the corresponding alcohol was observed (Table 5, entry 1). For sodium hydroxide, the conversion (50%, entry 2) is substantially higher, and even higher conversion was obtained when lithium hydroxide (55%, entry 3) was employed. The active catalyst should be the formed alkoxide, thus it was interesting to see if better results could be obtained when the alkali alkoxides were used directly. Using sodium *iso*-propoxide (6 mol %), indeed higher conversion (71%, entry 5) to the alcohol was obtained. When using instead potassium *tert*-butoxide, a drop in conversion (20%, entry 4) was the result. However when lithium *iso*-propoxide was employed, the conversion was restored (71%, entry 6). By increasing the reaction temperature to 180 °C, high conversion (96%, Table 6, entry 1) could be obtained in only 20 minutes.

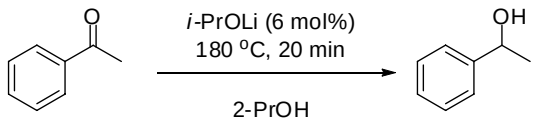


**Scheme 18.**

[89] a) Woodward, R. B.; Wendler, N. L.; Brutschy, F. J. *J. Am. Chem. Soc.* **1945**, *67*, 1425-1429; b) Doering, W. E.; Cortes, G.; Knox, L. H. *J. Am. Chem. Soc.* **1947**, *69*, 1700-1710; c) Doering, W. E.; Aschner, T. C. *J. Am. Chem. Soc.* **1949**, *71*, 838-840; d) Baramee, A.; Chaichit, N.; Intawee, P.; Thebtaranonth, C.; Thebtaranonth, Y. *J. Chem. Soc., Chem. Commun.* **1991**, 1016-1017

[90] a) Bagnell, L.; Strauss, C. R. *Chem. Commun.* **1999**, 287-288; b) Sominsky, L.; Rozental, E.; Gottlieb, H.; Gedanken, A.; Hoz, S. *J. Org. Chem.* **2004**, *69*, 149-1496

From these results it seems as if sodium and lithium are better than potassium for this reaction. Furthermore, the direct use of the alkali alkoxide seems to be most effective for good reactivity of the base.

From an experiment with 2-PrOD as solvent, it can be seen that no deuterium is transferred to the carbonyl carbon of the substrate. Thus, the reaction proceeds via a direct hydride transfer mechanism (Scheme 1).

**Table 5.** Catalytic results employing different alkali alkoxides for the reduction of acetophenone.[a]

| Entry | Alkali base | Conversion [%] |
|---|---|---|
| **1** | KOH | 15 |
| **2** | NaOH | 50 |
| **3** | LiOH | 55 |
| **4** | *t*-BuOK | 20 |
| **5** | *i*-PrONa | 71 |
| **6** | *i*-PrOLi | 71 |

a) Reaction conditions: acetophenone (1 eq, 0.2 M in 2-propanol), alkali base (6 mol%), 90 minutes at 120 °C.

## 5.2 The scope of the reaction

The influence of electronic effects of the substrate on the reaction outcome can be studied by performing the reaction on differently substituted acetophenones. Performing the reaction with *para*-bromo acetophenone results in lower conversion (88%, Table 6, entry 2). This can be explained by the lower electron density at the carbonyl which makes the coordination to the lithium weaker. This effect is smaller for the *ortho* and *meta*- bromo substituted acetophenone (93% and 96% respectively, entries 3-4), so it seems as if the electronic effect from having the substituent in the *para* position is larger than the steric effect from the *ortho* or *meta* substitution. When heating halobenzenes with strong nucleophilic bases, they can undergo nucleophilic aromatic substitution. In the case of the bromo substituted acetophenones, this side reaction was not observed. However, when using fluoro substituted acetophenones, this reaction occurred, so these types of substrates are not suitable for this protocol.

A substrate that is normally troublesome when using transition metal-based catalysts is the highly deactivated 4-cyano acetophenone. Coordination between the nitrile and the catalyst often inhibits the reaction. An efficient reduction to the alcohol is however achieved when the *i*-PrOLi protocol is used (entry 5).

Similar results are obtained when instead electron-rich substrates, such as methoxy substituted acetophenones, are used. With the methoxy group in the *ortho* or *para* position, the electron density is higher at the carbonyl, thus making the hydride attack less favored. Lower conversion was obtained for the *para*-methoxy as compared to the *ortho* or *meta*. Extended reaction time resulted in higher conversion for this substrate (entry 6).

More sterically hindered substrates such as *tert*-butyl phenyl ketone and benzophenone are efficiently reduced, although slightly longer reaction time is necessary (entries 9-10).

Acetyl pyridines have been problematic substrates in the aluminium mediated MVP reduction due to coordination between the nitrogen in the aromatic ring and the metal. These problems are overcome using the *i*-PrOLi protocol, and excellent results are obtained for the reduction of both 2- and 3-acetylpyridine (entries 12-13).

In the case of certain aliphatic substrates, e.g 5-nonanone and camphor, the reduction does not work properly. Only starting material and/or condensation products were detected in the reaction mixture. Other aliphatic ketones, such as cyclohexyl methyl ketone and 5α-cholestan-3-one are readily reduced to the corresponding alcohols (entries 14-15).

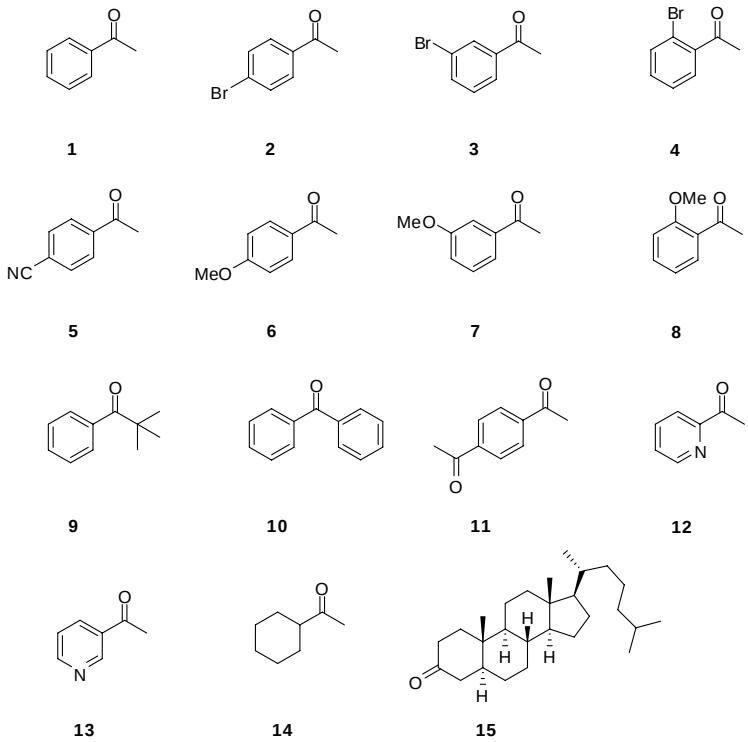


**Figure 20.** Ketones investigated in the *i*-PrOLi reduction. Number refer to the entries in Table 6.

**Table 6.** Catalytic results for the reduction of different ketones.[a]

| Entry | Time [min] | Conversion [%] | Isolated yield [%] |
|---|---|---|---|
| **1** | 20 | 96 | 94 |
| **2** | 20 | 88 | 83 |
| **3** | 20 | 96 | |
| **4** | 20 | 93 | |
| **5** | 20 | 96 | 87 |
| **6** | 30 | 86 | 80 |
| **7** | 20 | 92 | |
| **8** | 20 | 93 | |
| **9** | 30 | 96 | 87 |
| **10** | 30 | | 93 |
| **11** | 40 | 89 | 83 |
| **12** | 20 | 99 | 99 |
| **13** | 20 | 99 | 96 |
| **14** | 20 | 54 | |
| **15** | 20 | | 93 |

a) Reaction conditions: acetophenone (1 eq, 0.2 M in 2-propanol), *i*-PrOLi (6 mol%), 180 °C

## 5.3 Large scale experiment

It is also possible to perform this reaction on larger scales. Using the Advancer instrument from Biotage AB, the reaction was performed with 41 mmol of acetophenone and 6 mol% *i*-PrOLi as catalyst. This resulted in a conversion of 97% to the corresponding alcohol. Encouraged by this result, we doubled the amount of acetophenone to 82 mmol, hence using 3 mol% of catalyst. This time we got a conversion of 95% and an isolated yield of 89%.

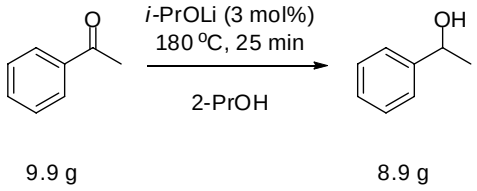


9.9 g 8.9 g

**Scheme 19.** Multigram scale reduction of acetophenone.

## 5.4 Conclusions

We have demonstrated that simple and inexpensive alkali alkoxides work as catalysts for transfer hydrogenation of various ketones in 2-PrOH via a MVPO-type mechanism. With microwave irradiation as heating source, this is a simple method with short reaction times. A parallel experiment with conventional heating has shown that there is no special microwave effect, but the use of microwave irradiation is convenient and gives good control of the reaction temperature. In summary, this protocol is a good complement to the use of $NaBH_4$ in the reduction of ketones to alcohols. It gives high conversions in relatively short reaction times and does not require any tedious workup.

# 6 Concluding remarks

With growing environmental awareness in our society, there is an increasing demand for the development of green chemistry methods. Catalysis using harmless chemicals is a good approach in the strive to minimize the use of toxic and environmentally hazardous material.

In the work presented in this thesis, the reducing abilities of several transition metal complexes are studied. In the first part, a closer look at the reasons behind the enantioswitchable properties of amino acid based rhodium complexes applied in asymmetric transfer hydrogenation is carried out. Small differences in the catalyst structure enable the production of both enantiomers of the substrate using amino acids available from the chiral pool.

When developing new catalysts, inspiration can be taken from natures catalytic systems. These are often highly efficient and selective, and are active under mild conditions. Inspired by the Fe hydrogenases, we studied the properties of a novel di-iron carbonyl complex with a labile amine ligand. This complex mimics a feature of the enzyme active site that has not been thoroughly investigated.

Further, with the aim of achieving light-induced hydrogen production, a di-iron carbonyl complex was coupled to a photosensitizer. This system is still in need of some fine-tuning, and the di-iron moiety needs to be more light-stable before the goal can be reached.

In the last part of this thesis, a catalytic protocol for the transfer hydrogenation of ketones without the involvement of transition metal catalyst is presented. With this method, a “greener” way of obtaining secondary alcohols from ketones is realized.

# Acknowledgements

Så var det över till slut. Det här har dock inte varit en enmansshow och jag skulle vilja passa på att tacka ett antal personer som bidragit på olika sätt.

För och främst skulle jag vilja rikta ett jättestort tack till min handledare *Hans Adolfsson*, för all inspiration, alla kloka råd, intressanta diskussioner samt för att du alltid tagit dig tid att besvara mina frågor.

Jag vill tacka *Björn Åkermark* och *Licheng Sun*, för att ni antog mig till forskarutbildningen och lät mig vara delaktig i ett mycket spännande projekt.

*Jan-Erling Bäckvall* för visat intresse i mina projekt.

Ett stort tack också till *Sascha Ott* för all hjälp med järn-projekten.

Alla medlemmar i BÅ-gruppen för en trevlig och stimulerande tid: *Henriette*, *Magnus*, *Olof*, *Yunhua*, *Jacob*, *Josefin*, *Sascha*, *Lennart*, *Hanna*, *Hoa*, *Susan*, *Gurra, Xiaobing Shiguo* och *Xichuan*

Alla medlemmar i HA-gruppen, för en mycket givande ”andra halvlek”: *Jenny*, *Katrin*, *Patrik*, *Alexey*, *Elina*, *Nisse*, *Lorenzo*, *Anders*, *Maria* och *Christopher.*

Konsortiet för Artificiell fotosyntes, särskilt *Maria*, *Carol*, *Leif* och *Reiner* för trevligt samarbete.

Mina samarbetspartners *Alexey*, *Jenny*, *Katrin*, *Lennart, Weiming* och *Henriette*.

*Lars Eriksson* och *Betul Kaynak* för hjälp med kristallstrukturer.

Grabbarna för lunch, poker, kryss, snappsprovning, m.m.

Tack till *Micke*, *Henke*, *Hoa*, *Lennart*, *Jenny* och *Jakob* för de roliga resorna till San F och Nara.

Alla nuvarande och tidigare medarbetare på Institutionen för Organisk kemi, för en rolig och inspirerande arbetsmiljö.

*Hasse, Katrin, Sascha, Jenny* och *Björn* för hjälp med korrekturläsning.

*Byron* för hjälp med språkgranskning.

*Per Unger* och *Bertil Erbing* för hjälp när det behövdes.

Tack till TA-personalen *Britt*, *Magnus*, *Olle*, *Pia*, *Kristina*, *Robin*, *Ola*, Agneta, *Daniel* och *Lilly* för hjälp med datorer, NMR, krånglande dragskåp, blanketter m.m.

*Hillevi* för hjälp i biblioteket.

*Jonas Hellberg*, *KZ*, *Peter Somfai* och *Pino* för att ni väckt mitt intresse för detta ämne.

Jag skulle vilja tacka *Svenska kemistsamfundet*, *Astrazeneca*, *Ångpanneföreningen* och *Liljevalchs J:ors stiftelse* för finansiellt stöd, samt *Gålö stiftelsen* för ekonomiskt stöd under min grundutbildning.

*Hammarby IF* och alla sköna bajare därute.

Tack till alla kompisar utanför universitetet, för att ni med jämna mellanrum dragit ut mig i verkligheten.

Serdecznie dziękuję moja rodzina w Polsce, och ett stort tack till familjen *Ahlford* också.

Tack till *mamma*, *pappa*, *Hasse* och *Britt-Mari* för allt stöd och uppmuntran under min studietid.

Slutligen så vill jag tacka *Katti* för all ovärderlig hjälp och ditt stora tålamod nu på slutet ♥